ISSN 0503-1540

Tome 20 *Février 1982* Numéro 1

La mer

うみ

昭和 57 年 2 月

日 仏 海 洋 学 会

La Société franco-japonaise
d'océanographie
Tokyo, Japon

日仏海洋学会

編集委員会

投稿規定

1. 報文の投稿者は本会会員に限る。
2. 原稿は簡潔にわかりやすく書き，図表を含めて印刷ページで**10**ページ以内を原則とする。原稿（正**1**通，副**1**通）は，（〒101）東京都千代田区神田駿河台2-3　日仏会館内　日仏海洋学会編集委員会宛に送ること。
3. 編集委員会は，事情により原稿の字句の加除訂正を行うことがある。
4. 論文（欧文，和文とも）には必ず約200語の欧文（原則として仏語）の要旨をつけること。欧文論文には欧文の要旨のほかに必ず約500字の和文の要旨をつけること。
5. 図及び表は必要なもののみに限る。図はそのまま版下になるように縮尺を考慮して鮮明に黒インクで書き，論文の図及び表には必ず英文（又は仏文）の説明をつけること。
6. 初校は原則として著者が行う。
7. 報文には1編につき50部の別刷を無料で著者に進呈する。これ以上の部数に対しては，実費（送料を含む）を著者が負担する。

RECOMMANDATIONS A L'USAGE DES AUTEURS

1. Les auteurs doivent être des membres de la Société franco-japonaise d'océanographie.
2. Les notes ne peuvent dépasser dix pages. Les manuscrits à deux exemplaires, dactylographiés sur papier fort, doivent être envoyés au Comité de rédaction de la Société franco-japonaise d'océanographie, c/o Maison franco-japonaise, 2-3, Kanda Surugadai, Chiyoda-ku, Tokyo, 101 Japon.
3. Le Comité de rédaction se réserve le droit d'apporter, le cas échéant, des modifications mineuses aux manuscrits ainsi que de demander aux auteurs de les corriger.
4. Des résumés en langue japonaise ou langue française sont obligatoires.
5. Les figures au trait seront tracées à l'encre de Chine noire sur papier blanc ou sur calque. Les légendes des figures et des tableaux sont indispensables.
6. Les premières épreuves seront corrigées, en principe, par les auteurs.
7. Un tirage à part des articles en cinquante exemplaires est offert gratuitement aux auteurs. Ceux qui en désirent un plus grand nombre peuvent les faire établir à leurs frais.

La mer 20: 1-8, 1982
Société franco-japonaise d'océanographie, Tokyo

Particle Size Distribution and Light Scattering in Akita Bay*

Ryohei TSUDA** and Kisaburo NAKATA***

Abstract: The volume scattering function and the size distribution of particles were measured in water samples which were taken from the surface and several layers of water in Akita Bay, northern Japan. Observed distribution over the size range of 2.3-18.8 μm approximated an exponential curve in June and a hyperbolic in November. Using these size distributions, the cross-section concentration in consideration of particles smaller than 2.3 μm was calculated, and the correlation between the cross-section concentration and the scattering coefficient was examined. As the result, it was found that the mean efficiency factor $\overline{Q}$ was in the ranges of 1.0-2.0 in June and 0.25-1.0 in November. From the correlation between the scattering coefficient computed from the size distribution and the volume scattering function, the indices of refraction of particles were estimated to be 1.02-1.05 in June and generally 1.05-1.10 in November. The percentage contribution of particles smaller than 2.3 μm to light scattering was computed as about 29 % in June and 33 % in November.

1. Introduction

The size of suspended particles in the sea varies over an extremely wide range of up to several hundred microns, and the size and quality of particles are closely related to light scattering. BEARDSLEY Jr., *et al.* (1970) found that both the light scattering at 45° and the total scattering coefficient were linearly related to total cross-section concentration of particles in the eastern equatorial Pacific. CARDER *et al.* (1971) related the particle concentration to the volume scattering function, β_{45} with depth and stated that the significant part of light scattering is due to small particles. As a result of measuring the volume scattering function and the size distribution of particles for certain surface waters of the North Pacific Ocean, SUGIHARA and TSUDA (1979) suggested that the major optical effect is due to particles smaller than 2.4 μm. On the other hand, JERLOV (1976) summarized measurements by several workers and argued that most of the optical effect results from particles larger than 2.0 μm in diameter. GORDON and BROWN (1972) and ZANEVELD and PAK (1973) presented methods for determining the refractive index from the observed data of size distribution and volume scattering function at 45°. CARDER *et al.* (1972) have also presented a technique for the estimation of indices of refraction of marine phytoplankton.

Particle size distribution measurement is simplified by using the Coulter Counter. BADER (1970) reported that cumulative distribution of particle number closely approximated a Junge curve and similar results were obtained in Osaka Bay by MATSUMOTO (1975) and in the Kuroshio region by MATSUIKE and MORINAGA (1977). On the other hand, PLANK *et al.* (1971) showed that the size distribution of particles in the North Pacific Ocean corresponds to an exponential function, and in the eastern equatorial Pacific CARDER *et al.* (1971) showed that the distribution of particle number approximates an exponential curve, but could be described better by the Weibull distribution.

In this paper, the volume scattering function and size distribution of particle numbers of water samples which were taken from the surface and several layers in Akita Bay near the

* Received December 13, 1980
** Department of Fisheries, Faculty of Agriculture, Kinki University, Kowakae 3-4-1, Higashi-Osaka, Osaka, 577 Japan
*** National Research Institute for Pollution & Resources, M.I.T.I., Yatabe, Tsukuba, Ibaraki, 305 Japan

Oga Peninsula were measured to obtain the characteristics of size distribution and the relation between particles and optical properties.

2. Measurements

Water sampling was made in June and November 1978. Measurements of particle size distribution were made with a Coulter Counter (Model Type ZB) with 100 μm aperture which counts particles between 2.3 and 36.2 μm in size. The measurements were made four times for each sample and an average value was adopted. The volume scattering function was measured with a photometer similar to the Brice-Phoenix light scattering photometer. The volume scattering function of the sample water at the wavelength of 546 nm was measured at intervals of 5° in the angular ranges of 25°–140° and the scattering coefficient b_p was estimated according to the method reported by SUGIHARA and TSUDA (1979) (see Appendix).

3. Results and Discussion

(*1*) *Particle size distribution*

As shown in Fig. 1, the stations are located in areas south of the Oga Peninsula in Akita Bay. As examples of cumulative distribution, the results obtained at Stns. 2 and 6 are shown in Fig. 2. In the range of 2.3–18.1 μm, the distribution at Stns. 2 and 6 in June is almost linear but at the same stations in November it becomes concave on a semi-log scale. Accordingly, the cumulative particle size distribution is assumed to fit the following expressions respectively:

$$N_{>D}(D)=Ne\cdot e^{-aD} \qquad (1)$$

$$N_{>D}(D)=Nh\cdot D^{-b} \qquad (2)$$

where $N_{>D}$ is the number of particles having diameter larger than D, and Ne, Nh, a, and b are parameters to be determined from the observed distribution above 2.3 μm. The values of the parameters determined from the observed distribution over the size range of 2.3–18.1 μm by means of the least squares method and correlation coefficient are shown in Table 1. The calculated correlation coefficient, r, is over 0.95 in both June and November. In June, the observed size distribution fits an exponential

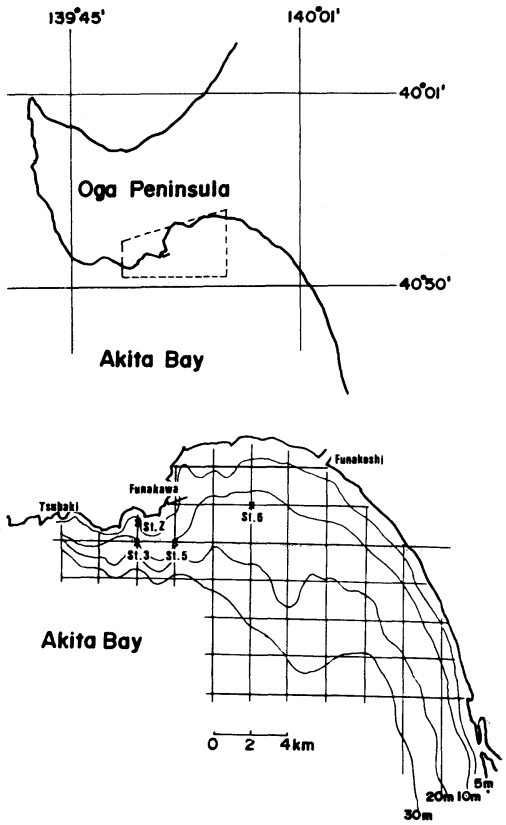

Fig. 1. Location of sampling stations in Akita Bay.

distribution described by Eq. (1) rather than a hypabolic one described by Eq. (2), except at a depth of one meter above the bottom where it becomes hyperbolic. This suggests that the number of small particles below 2.3 μm increases near the bottom. On the other hand, the observed distribution in November fits a hyperbolic shape better than an exponential, suggesting that a large number of small particles are present in Akita Bay. This problem will be discussed in the next section.

(*2*) *Particle scattering and properties*

The particle scattering is closely related to the particle number and the cross-section concentration of particles. It is important to examine the relationship between particle and optical properties. In the case of a polydispersed system, the scattering coefficient is yielded by

$$b_p=\frac{1}{4}\pi\sum_{i=1}^{n}Q_iN_iD_i^2, \qquad (3)$$

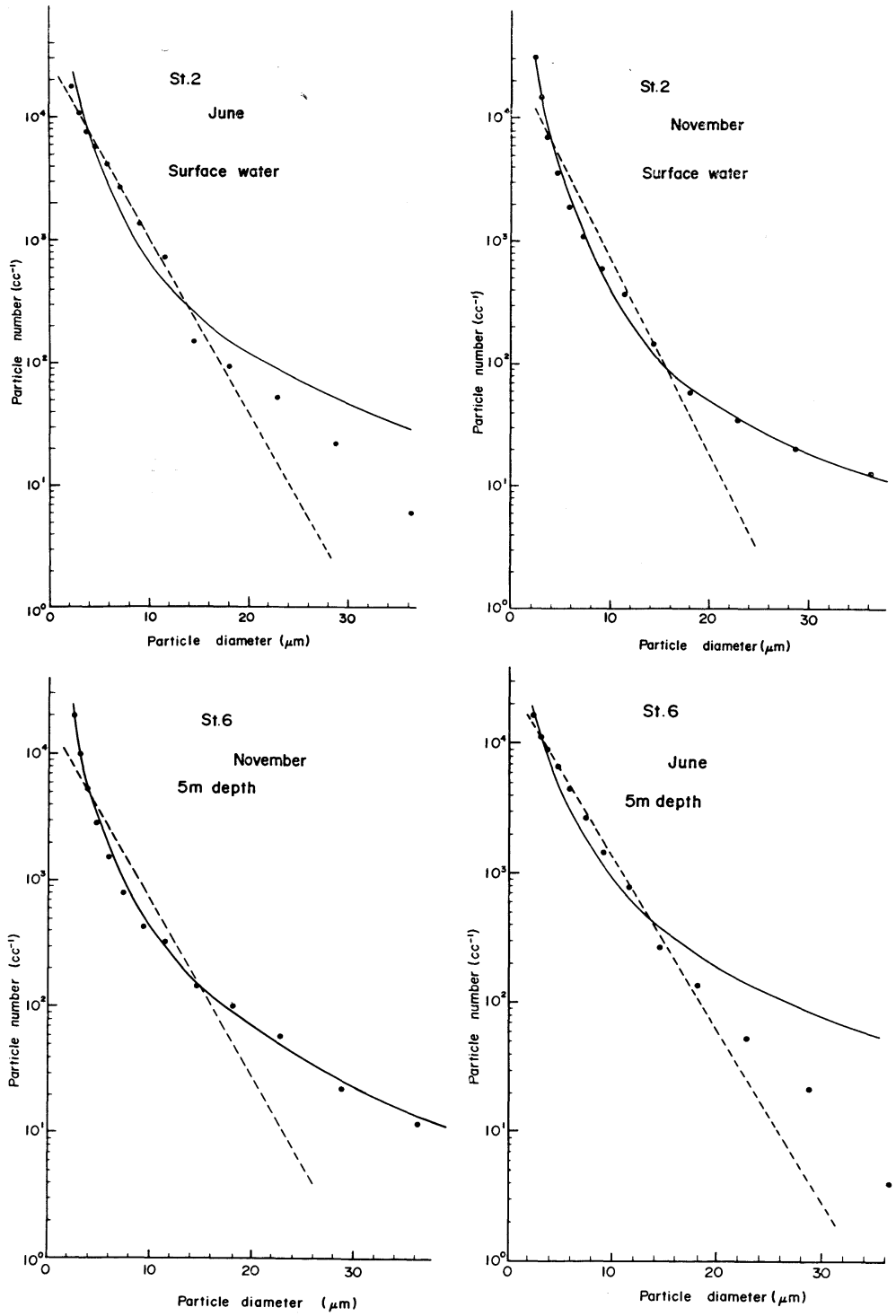

Fig. 2. Cumulative distribution of the particle number for water samples from Akita Bay. Dotted lines are exponential curves and solid ones are hyperbolic.

Table 1. Values of the parameters and the correlation coefficient (r) determined by the least squares method.

June 1978

Stn.	Depth (m)	$N_{>D}=Ne\cdot e^{-a\cdot D}$			$N_{>D}=Nh\cdot D^{-b}$		
		a	Ne	r	b	Nh	r
2	0	0.334	28957	−0.992	2.462	199638	−0.968
	1	0.338	31705	−0.992	2.508	229749	−0.973
	4	0.272	16271	−0.994	2.026	81442	−0.979
3	0	0.337	37433	−0.993	2.461	251557	−0.960
	5	0.346	44006	−0.992	2.594	352208	−0.983
	14	0.275	7581	−0.972	2.118	44046	−0.991
5	0	0.335	33141	−0.994	2.432	214266	−0.955
	1	0.326	28498	−0.986	2.460	208481	−0.985
	3	0.321	34212	−0.997	2.349	212332	−0.966
	5	0.317	25969	−0.997	2.296	150911	−0.957
	10	0.335	24480	−0.991	2.525	188402	−0.989
	12	0.324	16080	−0.994	2.420	111065	−0.983
	15	0.234	15521	−0.989	1.768	65250	−0.991
6	0	0.323	38888	−0.997	2.342	234954	−0.958
	5	0.305	26254	−0.996	2.257	155941	−0.977
	10	0.314	18878	−0.987	2.374	129865	−0.989

November 1978

Stn.	Depth (m)	$N_{>D}=Ne\cdot e^{-a\cdot D}$			$N_{>D}=Nh\cdot D^{-b}$		
		a	Ne	r	b	Nh	r
2	0	0.368	26586	−0.968	2.867	296904	−0.998
	1	0.344	34097	−0.971	2.674	320992	−0.998
	3	0.347	28467	−0.970	2.688	268862	−0.993
	4	0.371	46929	−0.979	2.855	499577	−0.997
3	0	0.335	20054	−0.961	2.603	178366	−0.989
	5	0.453	20192	−0.957	3.560	418091	−0.996
	12	0.330	16691	−0.959	2.556	141735	−0.984
5	0	0.310	14804	−0.939	2.486	129101	−0.997
	1	0.331	22975	−0.962	2.600	209278	−0.999
	3	0.332	21504	−0.972	2.581	187447	−0 999
	5	0.339	28666	−0.980	2.604	246408	−0.994
	10	0.350	35267	−0.990	2.624	290283	−0.993
	12	0.312	23145	−0.979	2.372	160687	−0.985
	13	0.293	21324	−0.967	2.278	144804	−0.996
6	0	0.395	37118	−0.981	3.027	452116	−0.996
	1	0.406	36197	−0.985	3.099	459317	−0.994
	5	0.322	15430	−0.946	2.567	141853	−0.998
	9	0.323	47203	−0.998	2.377	303822	−0.998

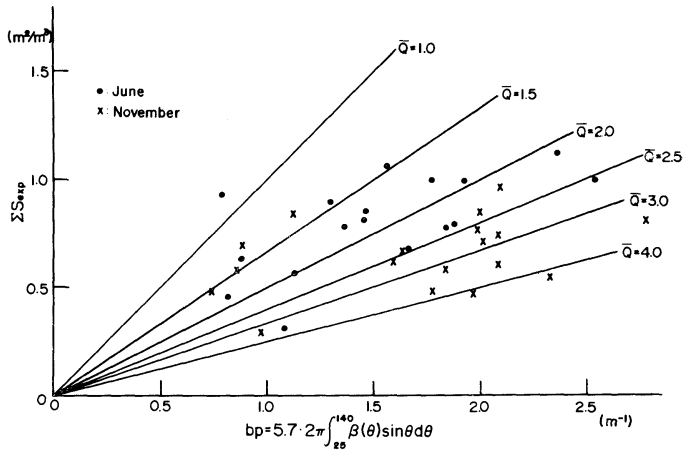

Fig. 3. Relationships between the cross-section concentration of particles larger than 2.3 μm and the scattering coefficient estimated from partial scattering coefficient for the wavelength of 546 nm.

where Q_i is the efficiency factor of the i-th particle and depends on the particle size, the refractive index and the wavelength of the scattered light.

The total cross-section concentration, $\Sigma S_{\exp}$, which can be calculated from the measured size distribution of particles is:

$$\Sigma S_{\exp}=\frac{1}{4}\pi\sum_{i=1}^{n}N_iD_i^2, \qquad (4)$$

where N_i is the number of particles of diameter D_i per unit volume. Fig. 3 shows the relationship between the total cross-section concentration of particles $\Sigma S_{\exp}$ and the scattering coefficient b_p estimated from b_p' at the wavelength of 546 nm (see Appendix). The correlation between b_p and $\Sigma_{\exp}$ is not good. The straight lines in the figure are drawn on the assumption that $\Sigma S_{\exp}$ is proportional to b_p for different efficiency factors. It is clearly seen from Eq. (3) and Eq. (4) that

$$b_p=\frac{\frac{1}{4}\pi\sum_{i=1}^{n}Q_iN_iD_i^2}{\frac{1}{4}\pi\sum_{i=1}^{n}N_iD_i^2}\cdot\Sigma S_{\exp}=\bar{Q}\cdot\Sigma S_{\exp}, \qquad (5)$$

where $\bar{Q}$ is the mean value of the efficiency factors. The points in June fall between two lines having slopes of 1.5 and 2.5 and those in November, 2.0 and 4.0. The value Q_i approaches 2 with increasing particle diameter and fluctuates between certain values as the particle size becomes smaller. Even if the refractive index of particles is 1.20, Q_i cannot take a value of more than 3.7 (SUGIHARA and TSUDA, 1979). The values in both June and November lie well within the prescribed range. We must also take into consideration the presence of particles smaller than 2.3 μm in the seawater. In the present case, the distribution of particle size is not known for particles smaller than 2.3 μm. It is evident from Table 1 that the observed size distribution between 2.3 and 18.1 μm is approximately hyperbolic or exponential in shape. Accordingly, these curves were assumed to be applicable for the calculation of particles smaller than 2.3 μm. From the extrapolated distribution thus obtained, we computed the number of particles smaller than 2.3 μm. The computation was carried out down to 1.0 μm and the contribution of particles smaller than that was neglected. The relationship between the total cross-section concentration of particles larger than 1.0 μm computed by Eq. (4) and the scattering coefficient estimated from measured partial scattering coefficient at the wavelength of 546 nm is shown in Fig. 4. The total cross-section concentration in November increases considerably with the contribution of small particles and most of the points are located between the two lines having slopes

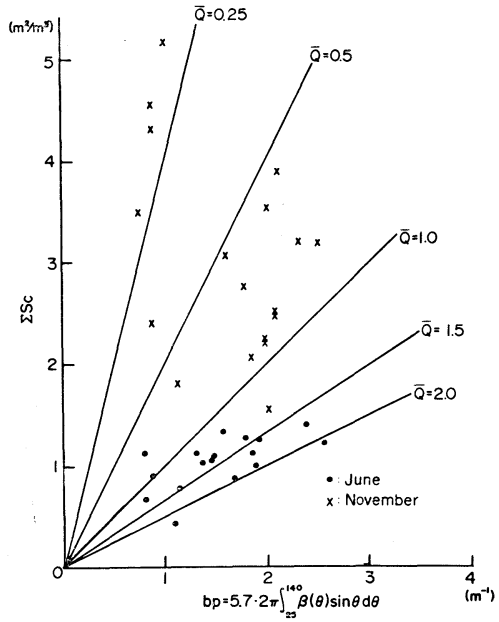

Fig. 4. Relationships between the cross-section concentration of particles larger than 1.0 μm and the scattering coefficient for the wavelength of 546 nm.

of 0.25 and 1.0, whereas those in June, 1.0 and 2.0. Judging from the fluctuation of Q, it is plausible that $\bar{Q}$ is less than 2. But the figure shows a considerable dispersion of plots. This is attributed to the over- and under-estimation in the number of small particles and also to the difference in the refractive index of the particles. The latter is especially relevant to scattering by particles.

In order to estimate the refractive index of particles in Akita Bay, we assumed the particles of non-absorbing spheres with refractive indices of 1.02, 1.05, and 1.10. The particle scattering coefficients were computed from the size distribution of particles by Eq. (3) and estimated from the partial scattering coefficient b_p* (see Appendix). Fig. 5 shows the relation of particle scattering coefficients estimated from size distribution to those estimated from a partial scattering coefficient. As is evident from Fig. 5, the refractive index in June is located in the range of 1.02–1.05 and it can be supposed that the suspended matter in Akita Bay contained a greater amount of organic matter as the values

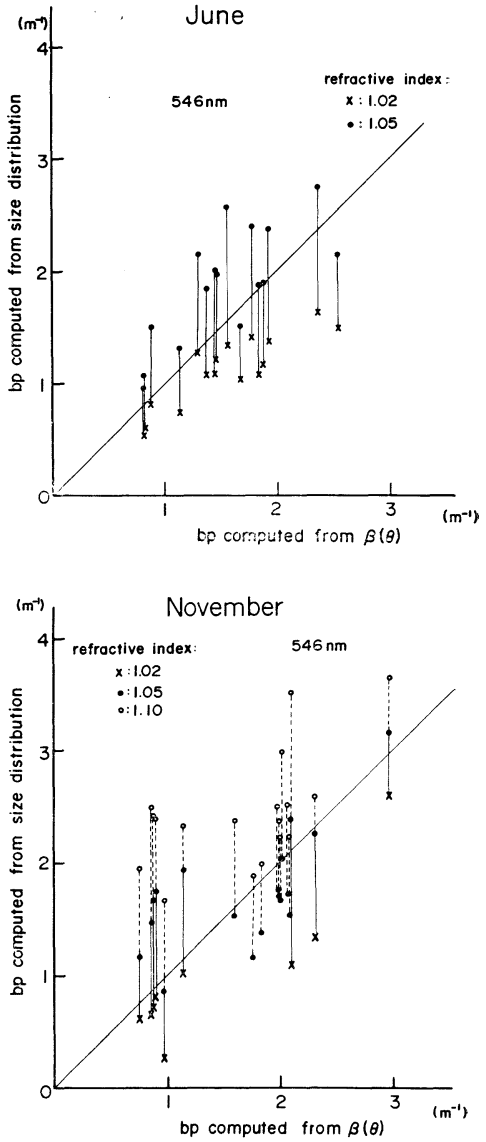

Fig. 5. Particle scattering coefficients computed from the size distribution of particles against those estimated from the partial scattering coefficient.

of the refractive indices approach unity. In November, it was considered nearly 1.05, but was not so clearly indicated as in June.

When refractive indices in June and November are assumed to be 1.02 and 1.05, the partial scattering coefficient, b_{po}, can be computed from the observed size distribution of particles between 2.3 and 36.2 μm. The contribution of

particles smaller than 2.3 μm to scattering was estimated from b_{po} and the scattering coefficient, b_p, was computed by Eq. (A-4) as follows:

$$\Delta b_p = \frac{b_p - b_{po}}{b_p}. \qquad (6)$$

The ratio takes the average value of 29 % (σ=0.133) in June and 33 % (σ=0.149) in November. The effect of particle scattering due to smaller particles in November is stronger than in June. OCHAKOVSKY (1966) found that about 70 % of the optical effect is caused by particles smaller than 1.0 μm, and similar results were also reported by LYSITSYN and BAGDANOV (1968) and BEARDSLEY, Jr., *et al.* (1970). The results of this study support those of previous studies that small particles have a significant optical effect and that the contribution of small particles to the scattering is significant. Accordingly, in order to clarify further the relationship between the optical properties and particles it is important to obtain more accurate information concerning the size distribution of small particles and the refractive index of those particles.

Acknowledgement

The authors would like to thank Dr. S. SUGIHARA and Mr. M. KISHINO, the Institute of Physical and Chemical Research, who kindly helped them in measuring the volume scattering function.

References

BADER, H. (1970): The hyperbolic distribution of particle size. Jour. Geophys. Res., **75**, 2822-2830.

BEARDSLEY, Jr., G.F., H. PAK and K. CARDER (1970): Light scattering and suspended particles in the eastern equatorial Pacific Ocean. Jour. Geophys. Res., **75**, 2833-2845.

CARDER, K.L., G.F. BEARDSLEY, Jr. and H. PAK (1971): Particle size distribution in the eastern equatorial Pacific. Jour. Geophys. Res., **76**, 5070-5077.

CARDER, K.L., R.D. TOMLINSON and G.F. BEARDSLEY, Jr. (1972): A technique for the estimation of indices of refraction of marine phytoplankton. Limnol. Oceanogr., **17**, 833-839.

GORDON, H.R. and O.B. BROWN (1972): A theoretical model of light scattering by Sargasso Sea particulates. Limnol. Oceanogr., **17**, 826-832.

JERLOV, N. G. (1976): Marine Optics. Elsevier, Amsterdam. 231 pp.

LISITSYN, A.P. and Y. BAGDANOV (1968): Granular composition of suspended matter in the Pacific Ocean. *In*, Oceanographic Research Collection 18. Science Publishers, Moscow. p. 53-74. (In Russian).

MATSUMOTO, E. (1975): Distribution of suspended particles in Osaka Bay. Kagaku, **45**, 177-188 (In Japanese).

MATSUIKE, K. and T. MORINAGA (1977): Beam attenuation and particle-size distribution in the Kuroshio area. La mer, **15**, 82-93.

MOREL, A. (1974): Optical properties of pure water and pure sea water. *In*, Optical Aspects of Oceanography (ed. by N.G. JERLOV and E. STEEMANN NIELSEN). Academic Press, London and New York. p. 1-24.

OCHAKOVSKY, Y. (1966): On the dependence of the total attenuation coefficient upon suspensions in the sea. U.S. Dept. Comm., Joiny Publ. Res. Rep., **36**, 98-105.

PETZOLD, T.J. (1972): Volume scattering function for selected ocean waters. SIO Ref., 72-28, p. 1-79.

PLANK, W.S., H. PAK and J.R. ZANEVELD (1972): Light scattering and suspended matter in nepheloid layer. Jour. Geophys. Res., **77**, 1689-1694.

SUGIHARA, S. and R. TSUDA (1979): Light scattering and size distribution of particles in the surface waters of the North Pacific Ocean. Jour. Oceanogr. Soc. Jap., **35**, 82-90.

ZANEVELD, J.R. and H. PAK (1973): Method for the determination of the index of refraction of particles suspended in the ocean. Jour. Opt. Soc. Amer., **63**, 321-324.

Appendix

The scattering coefficient b_p is obtained by integration,

$$b_p = 2\pi \int_0^{\pi} \beta(\theta) \sin\theta \, d\theta . \qquad (A-1)$$

The partial particle scattering coefficient b_p* in angular range 25° and 140° is calculated by subtracting the theoretical value for pure water $\beta_0(\theta)$ which was reported by MOREL (1974) from volume scattering function $\beta(\theta)$. Thus,

$$b_p^* = 2\pi \int_{25}^{140} \beta(\theta) \sin\theta d\theta - 2\pi \int_{25}^{140} \beta_0(\theta) \sin\theta d\theta . \qquad (A-2)$$

And if we assume that b_p and b_p* are linearly related, b_p is then given by

$$b_p = k \times b_p^*. \qquad \text{(A-3)}$$

The estimation of ratio b_p/b_p* was made using the values of volume scattering function observed in various regions by PETZOLD (1972). The computed values of b_p/b_p* were in the range from 5 to 6.5 with an average value of 5.7. Using this average value, the scattering coefficient b_p was estimated and given by

$$b_p = 5.7 \times b_p^*. \qquad \text{(A-4)}$$

秋田湾における懸濁物粒径分布と光散乱

津田良平, 中田喜三郎

要旨: 1978年6月および11月，秋田湾において採水された試料を用いて，海水中の懸濁物粒径分布と体積散乱函数の測定を行った。粒径 2.3～18.8 μm の測定範囲内では，その粒径分布は6月で指数分布，11月でべき乗分布として近似出来た。これらの粒径分布を用いて 2.3 μm 以下の小粒子を考慮した散乱断面積濃度を求め，これと散乱係数との相関を調べた．その結果，個々の平均散乱効率 $\overline{Q}$ の値は，6月は 1.0～2.0，11月は 0.25～1.0 の範囲であることがわかった。粒径分布と体積散乱函数から求めた散乱係数の相関から懸濁物の相対屈折率を調べると，6月は 1.02～1.05 付近にあると推定できたが，11月はほぼ 1.05～1.10 と考えられる。また，2.3 μm 以下の小粒子の散乱に寄与する割合いを計算すると，6月で 29 %，11月で 33 % となった。

La mer 20: 9-20, 1982
Société franco-japonaise d'océanographie, Tokyo

Current Measurements off Iriomote Island*

Hidetaka FUTI**, Magoshichi SATO**, Hideo INABA**,
Koki KAWABATA** and Yasuko TSUJI**

Abstract: Current measurements by using Aanderaa current meters were carried out from early November 1978 to early March 1979 near Iriomote Island. A mooring line equipped with current meters at 300 and 700 m below the sea surface was buoyed upward from a weight on the sea bottom by a buoy cluster. Two timed releases were attached to the lower end of the line. A back-up rope on the ground was attached above the releases and was moored by a mushroom anchor.

Spectral analysis of the current variations shows that the most prominent peak corresponds to the semidiurnal period and the secondary peak corresponds to the diurnal period. Almost no inertial period is found. Harmonic analysis of the four major tidal constituents shows the order of magnitude of the amplitude to be $M_2 > S_2 > K_1 > O_1$, just as the order of the amplitude of the surface elevation at Ishigaki Harbor near the mooring location. The phase difference of the M_2 constituent between 300 and 700 m was about 90°, suggesting that the tidal structure in this area was internal mode. The current speeds averaged over 25 hours varied greatly from 0 to 1.5 knots with periods from several days to a month.

1. Introduction

One of the most famous boundary currents of the great oceans, the Kuroshio, flows into the East China Sea through the strait between Taiwan and Yaeyama Islands. In order to investigate the characteristics of current variations, i.e. mean current and tidal current, in the sea near the Kuroshio path at the southernmost part of the East China Sea, current measurements by moored current meters were carried out in the sea to the northwest of Iriomote Island, one of Yaeyama Islands. A study of current pattern in the sea near the present mooring location was based on the estimation from the distributions of temperature and salinity (UDA, 1934), though particular attention was not paid to this area. Vertical profiles of current speed between Taiwan and Yaeyama Islands from dynamic calculations were studied by CHU (1976). According to his result, the Kuroshio flows with considerable width between Taiwan and Yaeyama Islands, and the axis of the Kuroshio is fixed near Taiwan and there frequently exist eddies or countercurrents of the Kuroshio near Yaeyama Islands.

The details of the measuring methods and the outlines of the obtained results will be described in this paper. The present investigation was carried out as a part of KER (Kuroshio Exploitation and Utilization Research).

2. Methods of measurement

a) Location, depth and duration of measurements

The location of the measurements is shown in Fig. 1. As can be seen in this figure, the location is to the northwest of Iriomote Island. The mooring location is about 1000 m deep. Its latitude and longitude are 24°24.2′N and 123°36.0′E. The topography near the mooring station is not flat; the depth increases downstream.

The current meter depths were 100, 300 and 700 m. Unfortunately, the current meter at 100 m flowed away before the recovery of the mooring system; therefore, the depths of the current measurements were 300 and 700 m. The current measurements were continued for 121

* Received May 28, 1981
** Institute of Oceanic Research and Development, Tokai University, Orido 1000, Shimizu, Shizuoka, 424 Japan

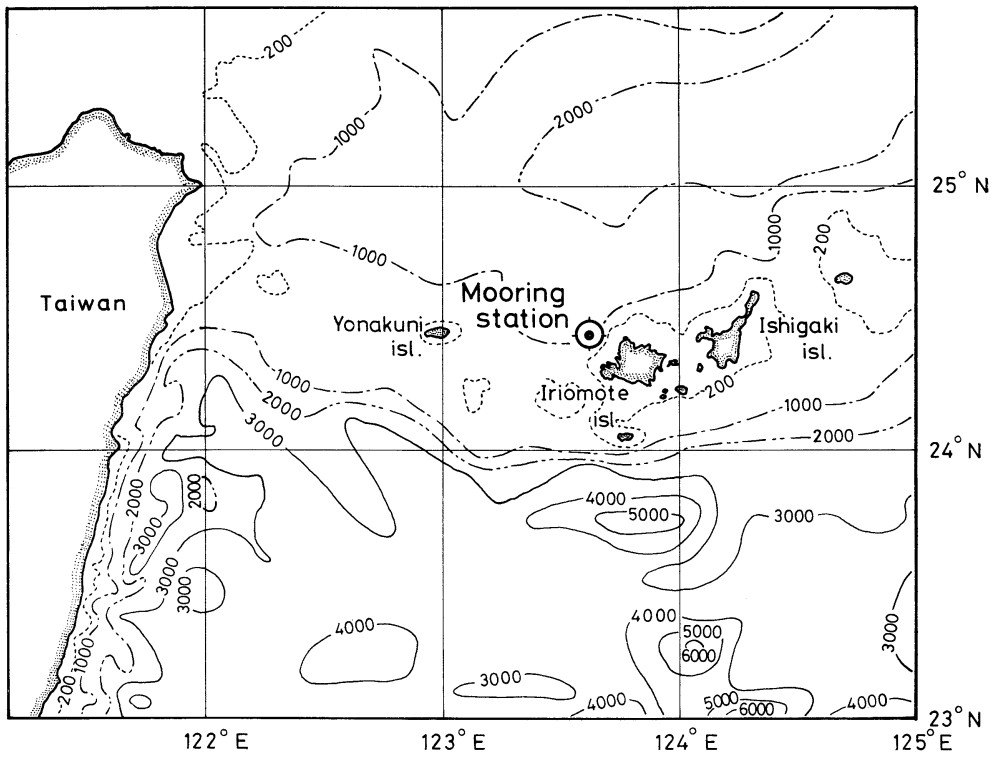

Fig. 1. Location of mooring station and isobathes (m).

days from November 3, 1978 to March 4, 1979.

b) Mooring system

The mooring system is illustrated in Fig. 2. The outline of the system is that two mooring lines, line A and line B, provide buoyancy by a buoy cluster and are connected to each other with a back-up long rope.

Line A is buoyed upward (270 m from the sea surface) by a buoy cluster. Two timed releases linked in parallel are attached to the lower end of the line. The buoy cluster consists of nine ABS resin floats. Its buoyancy is 321 kg. The rope between 300 and 700 m depths consists of a stainless wire rope of 6 mm in diameter. A nylon rope of 20 mm in diameter and 200 m in length is used below 700 m depth. To decrease the inclination of the mooring line at the current meter depth, two small buoys are attached just above the current meter at 700 m. The weight of rails, an anchor and a chain is about 600, 75 and 90 kg, respectively.

Line B, similar to line A, is buoyed upward (80 m from the sea surface) by a buoy cluster; a timed release is attached to the lower end of the line. The current meter is attached at a depth of 100 m. The buoy cluster consists o eight ABS resin floats. Its buoyancy is 286 kg.f The rope between 100 and 300 m depths is a nylon rope of 16 mm in diameter and 200 m in length. The rope below 300 m depth consists of a nylon rope of 16 mm in diameter and 650 m in length. The weight of rails, an anchor and a chain is about 500, 75 and 90 kg, respectively.

A back-up rope on the ground was a pylen rope of 20 mm in diameter and 2,580 m in length, and was attached above the releases of lines A and B. The rope was moored by a mushroom anchor (100 kg) at the middle and cement-mortar-block weights were attached at about 300 m intervals. The back-up rope on the ground could be retrieved with a grapnel if two releases acted before the preset time or if we could not arrive at the mooring position because of prohibitive sea conditions.

c) Instruments

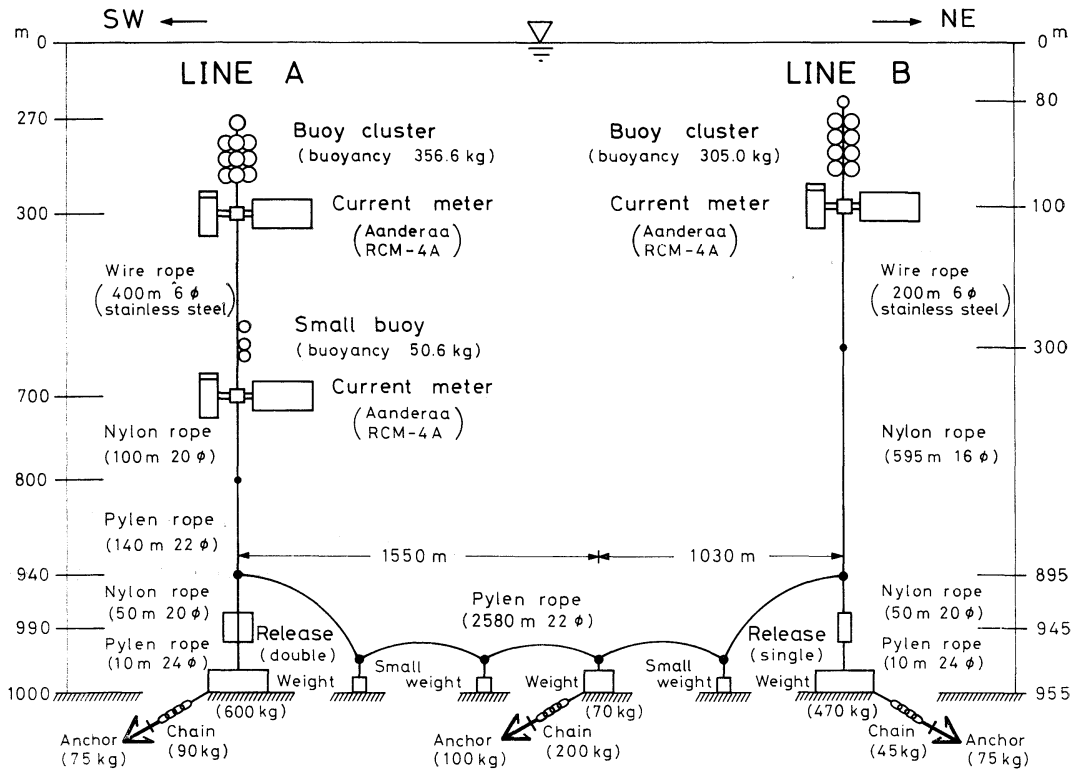

Fig. 2. Schematical sketch of the mooring system.

The three current meters, Bergen model-4, were equipped with temperature, salinity and pressure sensors. They measured average speeds over the sampling intervals (30 minutes in the present case) and instantaneous current directions, temperature, salinity and pressures.

The timed releases, model KT-1, were manufactured by Kaihatsu-Kogyo Co., Ltd. Two timed releases at line A and one at line B were used.

d) Deployment and recovery of the mooring system

The mooring system was deployed on November 3, 1978, from the Tokai Daigaku Maru II (702 ton), research and training ship of Tokai University. The deployment operation was done by lowering the buoy cluster first, followed by mooring lines and current meters of line A into the sea, while the ship was moving slow in the NE direction against the wind. The weight of line B was cast into sea and freely fell to the sea bottom, while the mooring rope of line B was quickly cast out. The buoy cluster at the upper end of line B was tightly held and pulled up by the ship going in the NE direction against the wind; finally, the buoy cluster was released and cast into sea.

The timed releases had been preset to 10:00 a.m. on March 4, 1979. The buoy cluster of line A was discovered 10 minutes after the preset time, but the buoy cluster of line B was not discovered immediately. Line A was buoyed upward to the sea surface and half of the back-up rope on the ground was recovered easily, but the remaining half of the back-up rope on the ground and the weight of line B were recovered with hardship due to the weight of line B. Unfortunately, no current meter on line B at 100 m depth was found due to the breaking of the mooring line just below the current meter. One month before the recovery of the mooring system, Bosei Maru II (1,218 ton), another research and training ship of Tokai University, had come to the mooring

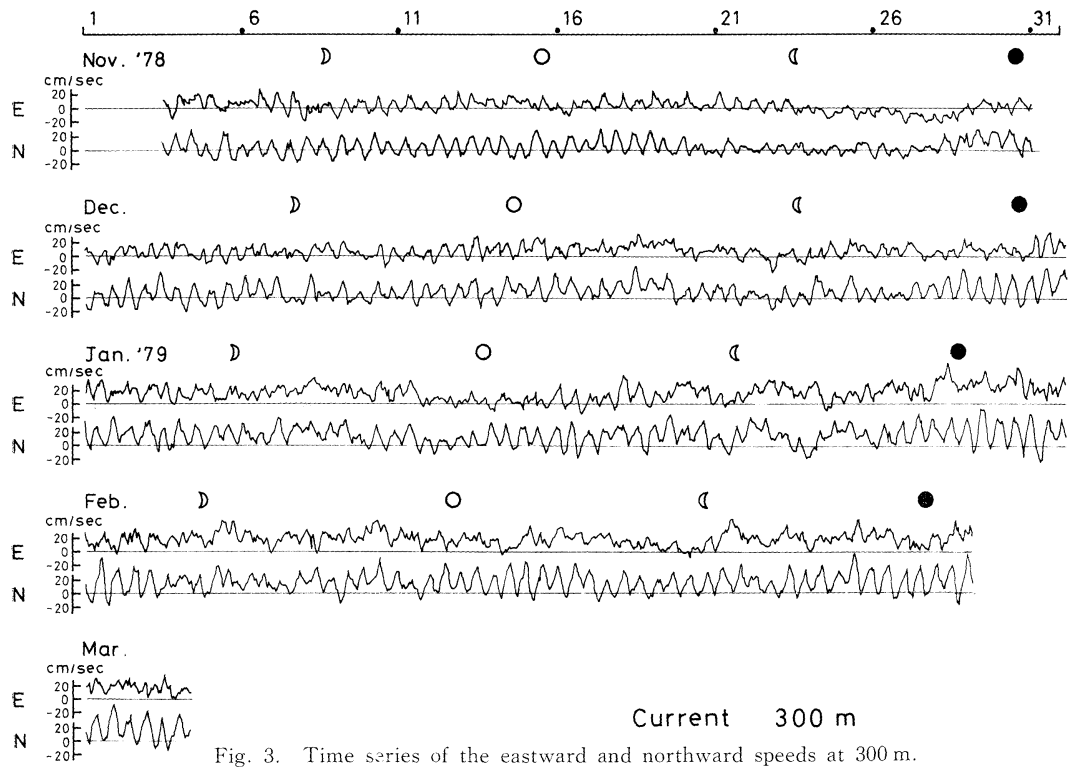

Fig. 3. Time series of the eastward and northward speeds at 300 m.

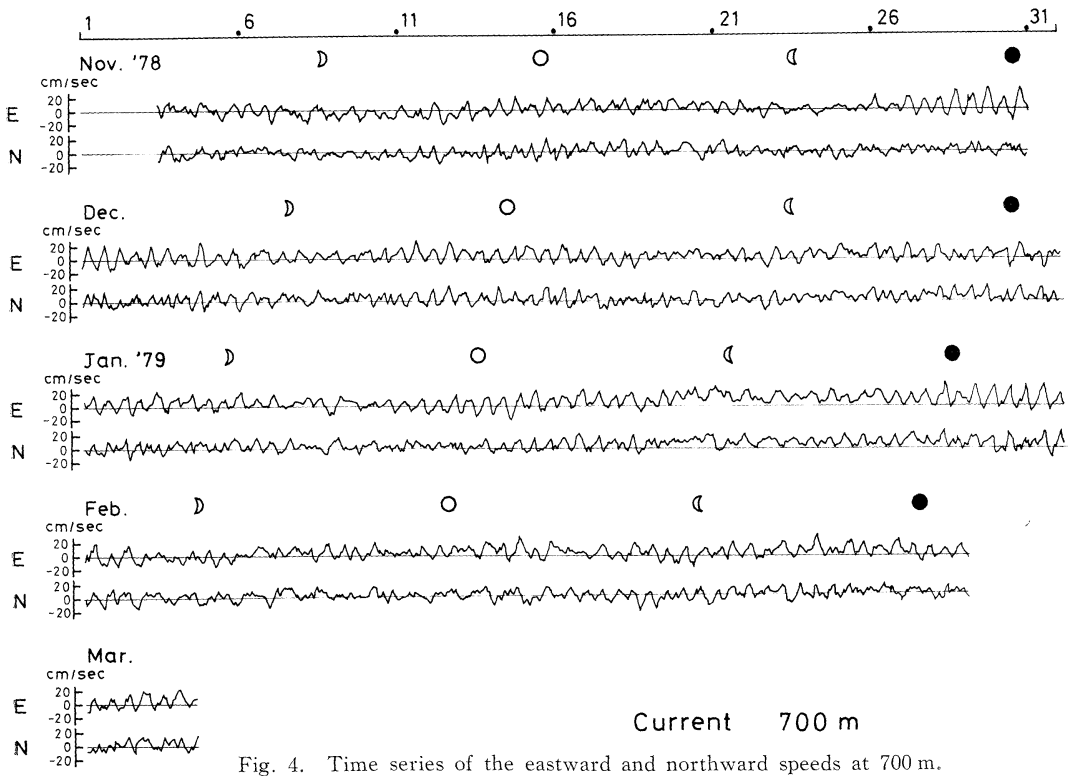

Fig. 4. Time series of the eastward and northward speeds at 700 m.

station and sonic signals of the current meters were recovered with a hydrophone receiver.

3. Results of measurements

a) Time series of currents

The time series of the eastward and northward components at 300 and 700 m are shown in Figs. 3 and 4. Fluctuations of the semidiurnal tidal current dominate through the whole period, accompanied with long-term variations. The amplitude of the tidal current changed remarkably with the phase of the moon. The phase of the semidiurnal constituent of the current at 700 m seems to lead that at 300 m by about 90°.

As to the mean current, the eastward and northward components are, though very weak, always positive. The mean currents at 300 and 700 m are in the NE direction.

b) Time series of temperatures

The time series of temperature at 300 and 700 m are shown in Figs. 5 and 6. Fluctuations of the semidiurnal tidal frequency dominate through the whole period, accompanied with long-term variations, similar to the fluctuations

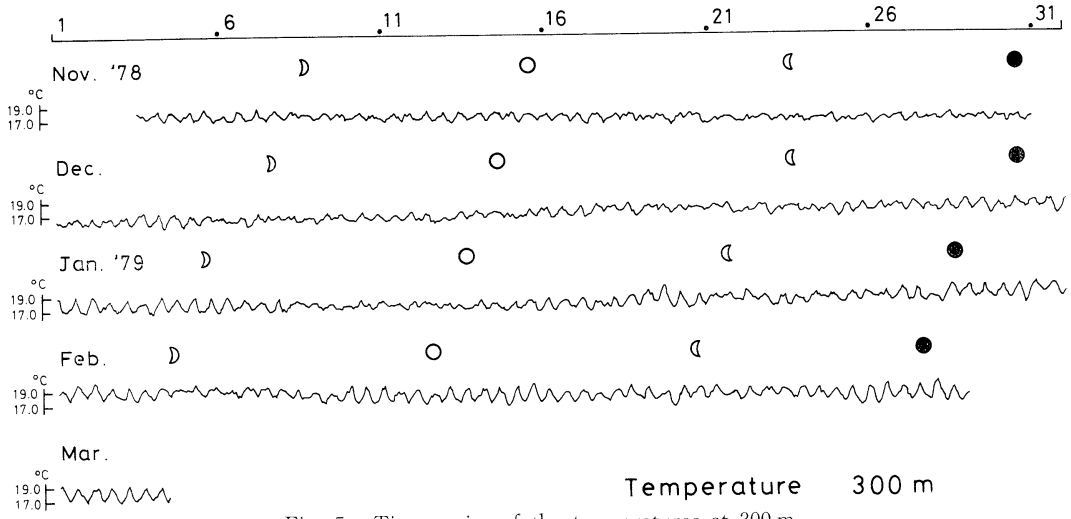

Fig. 5. Time series of the temperatures at 300 m.

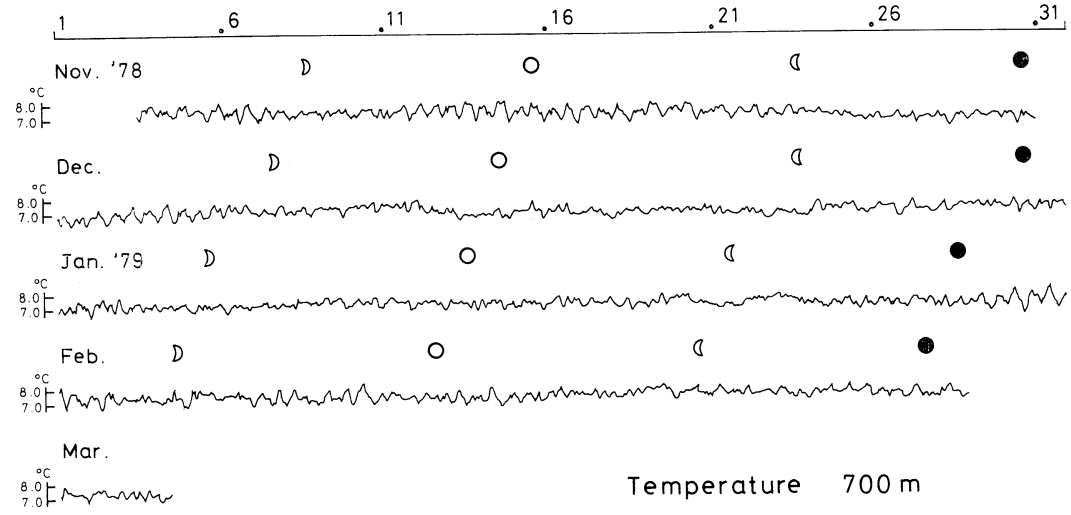

Fig. 6. Time series of the temperatures at 700 m.

of the current. The semidiurnal tidal amplitude at 300 m is much larger than that at 700 m. The phase of the semidurnal constituent of the temperature at 700 m seems to lead that at 300 m. The fluctuations of mean temperature become large in February and March.

c) Time series of salinities

The time series of salinity at 300 and 700 m are shown in Figs. 7 and 8. It can easily be seen in each figure that fluctuations of the semidiurnal tidal frequency dominate through the whole period, accompanied with long-term variations, similar to the fluctuations of the current and the temperature.

d) Pressure data at 300 m

Most values of the depth data were distributed between 281.19 and 306.63 m. Very few values were much larger than 290.40 m (56 samples out of 5808). Those at 700 m were distributed between 697.29 and 713.31 m, most of which are between 697.29 and 704.15 m. Very few values are larger than 713.13 m (26 samples out of 5808). The influence of the depth fluctuations on the current and the temperature is thought to be very small.

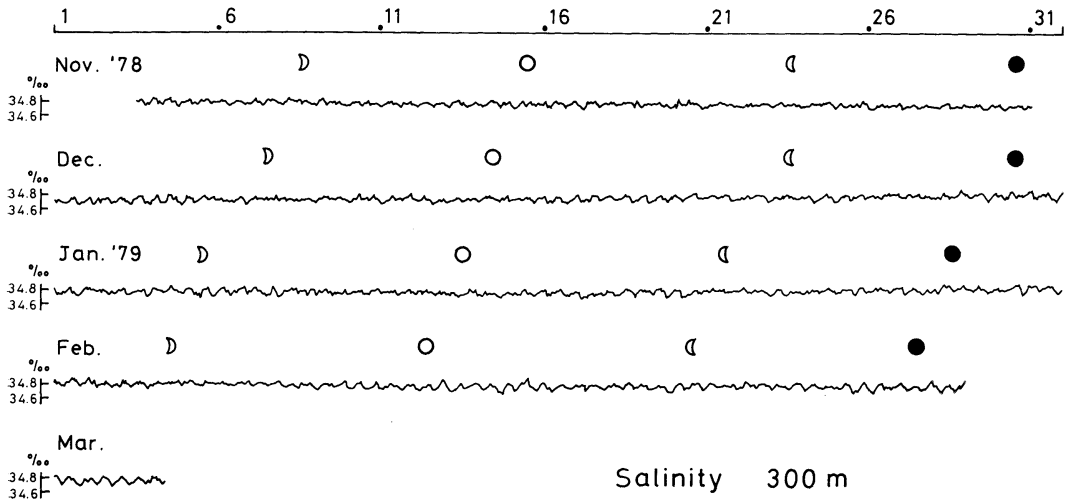

Fig. 7. Time series of the salinities at 300 m.

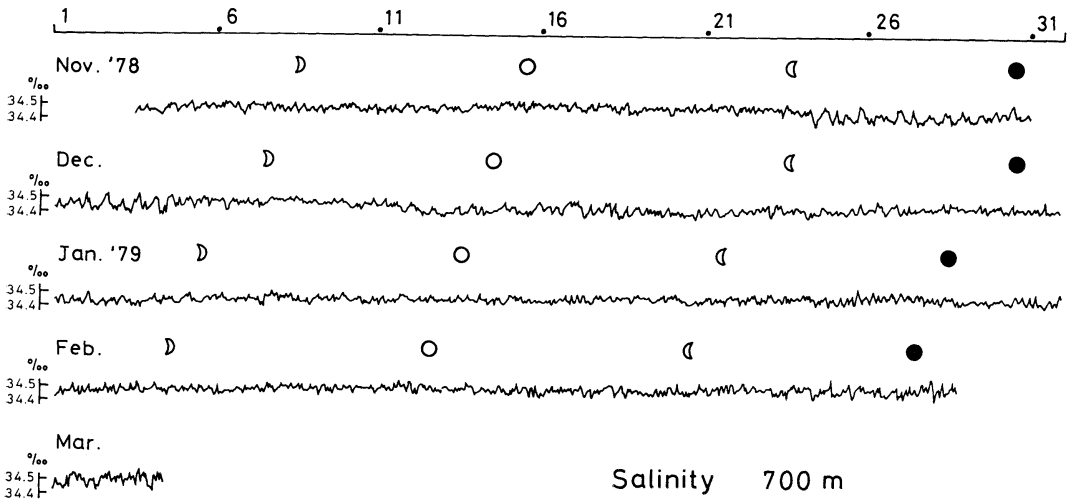

Fig. 8. Time series of the salinities at 700 m.

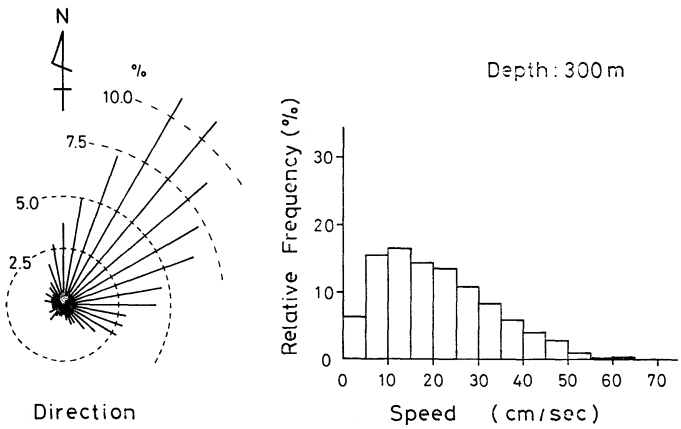

Fig. 9. Relative frequency distributions of the current directions and speeds at 300 m.

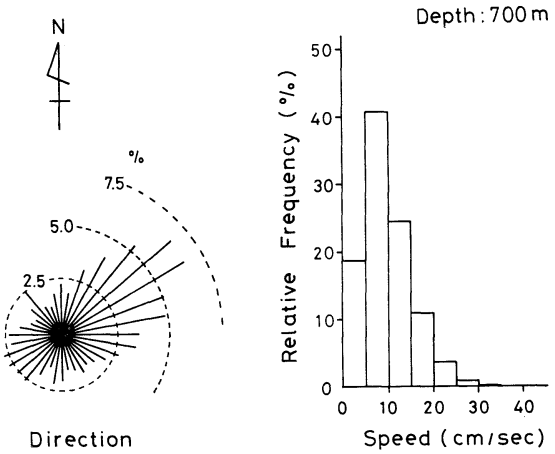

Fig. 10. Relative frequency distributions of the current directions and speeds at 700 m

4. Frequency distributions of the current speed and direction

The relative frequency distributions of the current speed and direction at 300 m are shown in Fig. 9. The current speeds from 10 to 15 cm/sec were dominant, though they varied from 0 to 65 cm/sec. Current directions from 30 to 40° were dominant; the opposite directions were seldom found.

The relative frequency distributions of the current speed and direction at 700 m are shown in Fig. 10. The current speeds from 5 to 10 cm/sec were dominant (about 40 %); they varied between 0 and 30 cm/sec. The current directions from 50 to 60° were dominant, but those in opposite directions were found. It is the mean current that was dominant at 300 m. The tidal current was dominant at 700 m.

5. Spectral structures of the current, temperature and salinity

Spectral analyses of the time series of the current, temperature and salinity were carried out by BT method in order to find the dominant periods of each variable. The spectra of the eastward and northward components of current at 300 and 700 m are shown in Figs. 11 and 12. The spectra of the temperature and salinity at 300 and 700 m are shown in Figs. 13 and 14. The energy density distributions have significant

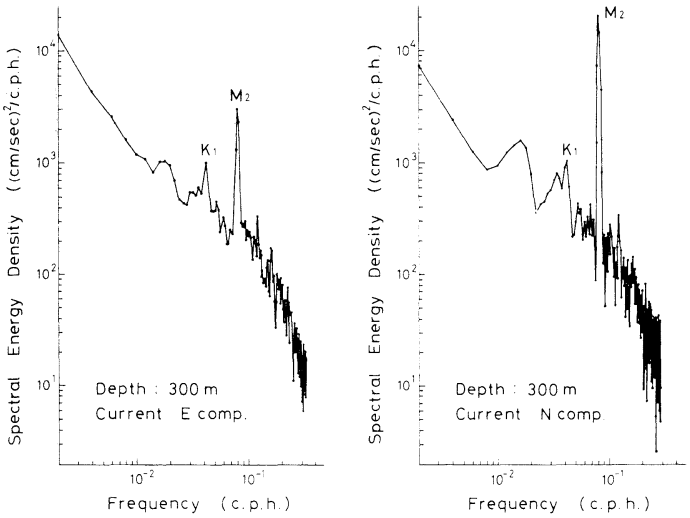

Fig. 11. Spectra of the velocities at 300 m.

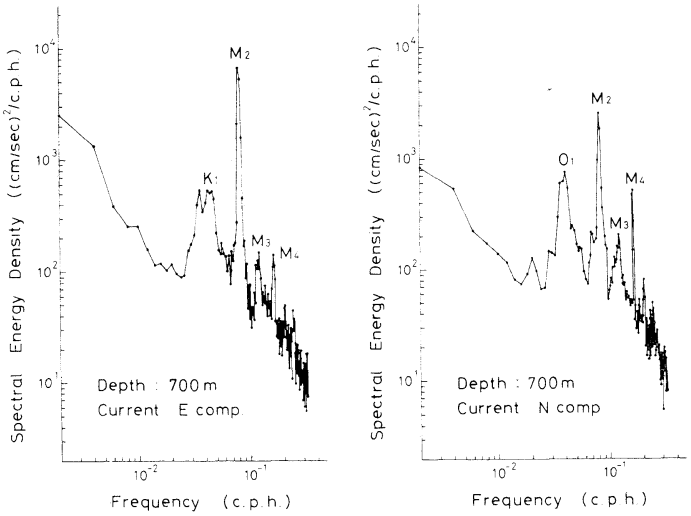

Fig. 12. Spectra of the velocities at 700 m.

features common to all of the calculated spectra. The most prominent peak corresponds to the semidiurnal period and the secondary peak corresponds to the diurnal period. The shallow-water tides (M_3, M_4) are clearly found in the spectra of the current, temperature and salinity at 700 m. The inertial period at 24°N is about 29 hours, but no distinct peak is found in these spectra. The spectral density in the frequency range lower than tidal frequency is very large and there exist a few peaks; their frequencies and powers differ from each other. The spectral density in the frequency range higher than tidal frequencies decreases with frequency according to the minus-five-thirds power law.

6. Tidal variations of the current and the temperature

The harmonic analyses for the four major tidal constituents, M_2, S_2, K_1 and O_1, of the current,

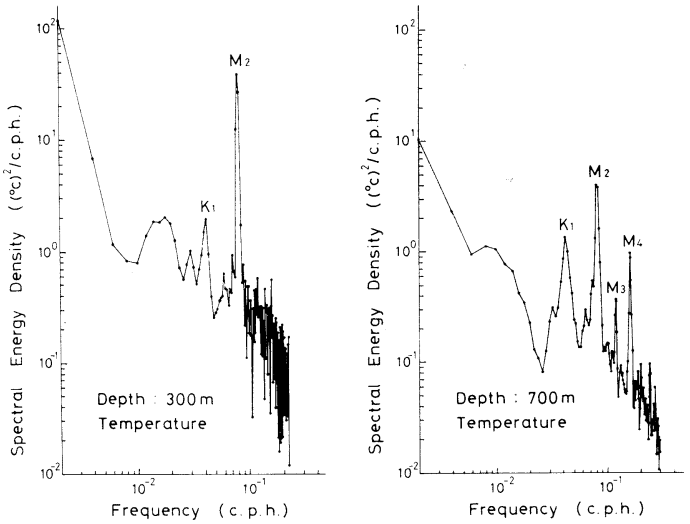

Fig. 13. Spectra of the temperatures at 300 and 700 m.

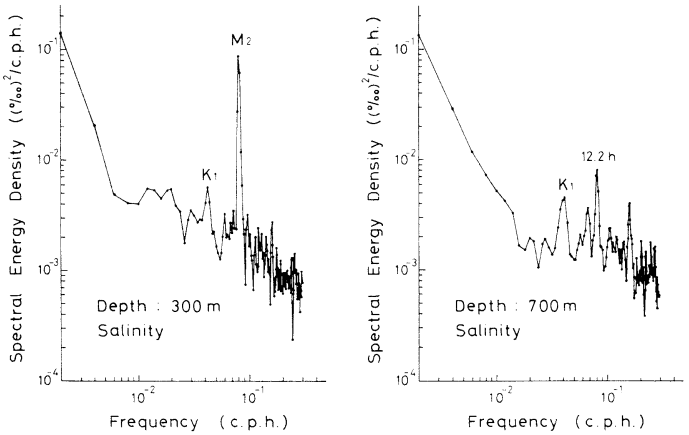

Fig. 14. Spectra of the salinities at 300 and 700 m.

Table 1. Harmonic constants of the four major tidal constituents of currents.

			Amplitude H (cm/sec, °C, ‰)				Phase Lag K(°)			
			M_2	S_2	K_1	O_1	M_2	S_2	K_1	O_1
	Current	E	3.57	0.64	1.80	0.36	276	143	101	355
		N	12.14	4.01	2.13	0.91	211	35	67	163
300 m	Temperature		0.542	0.118	0.072	0.037	80	76	65	198
	Salinity		0.029	0.006	0.007	0.008	309	249	18	193
	Current	E	6.83	2.61	0.77	0.17	116	282	9	111
		N	4.10	1.14	0.46	0.70	99	275	194	63
700 m	Temperature		0.109	0.071	0.063	0.006	273	231	47	291
	Salinity		0.004	0.002	0.003	0.001	293	338	320	92

temperature and salinity are carried out by the least square method and are shown in Table 1. The phases of the maximum are measured from the time of meridian passage of the fictitious heavenly bodies (125°E). As can be seen in the table, the amplitudes of semidiurnal constituents for three elements (current, temperature and salinity) are larger than those of the diurnal tidal constituents. The harmonic constants of the four major tidal constituents for the surface

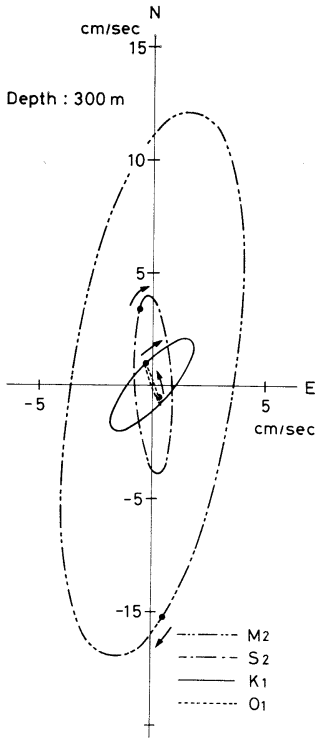

Fig. 15. Tidal ellipses of the four major tidal constituents at 300 m.

Table 2. Harmonic constants of the four major tidal constituents for the surface elevations at Ishigaki Harbor (NAKANO, 1940).

Constituent	Amplitude (cm)	Phase (°)
M_2	46	193
S_2	20	220
K_1	20	220
O_1	17	200

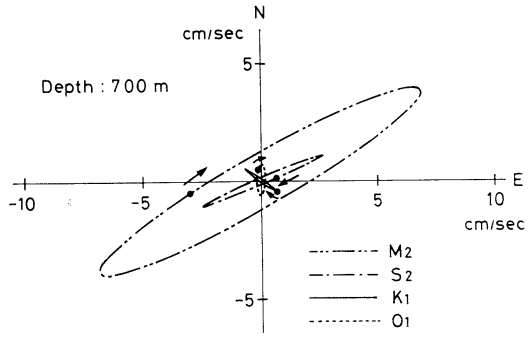

Fig. 16. Tidal ellipses of the four major tidal constituents at 700 m.

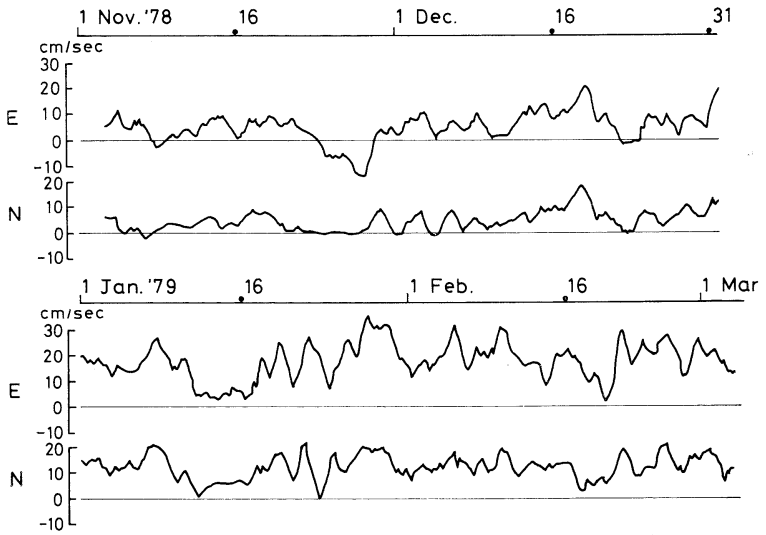

Fig. 17. Current speeds averaged over 25 hours at 300 m.

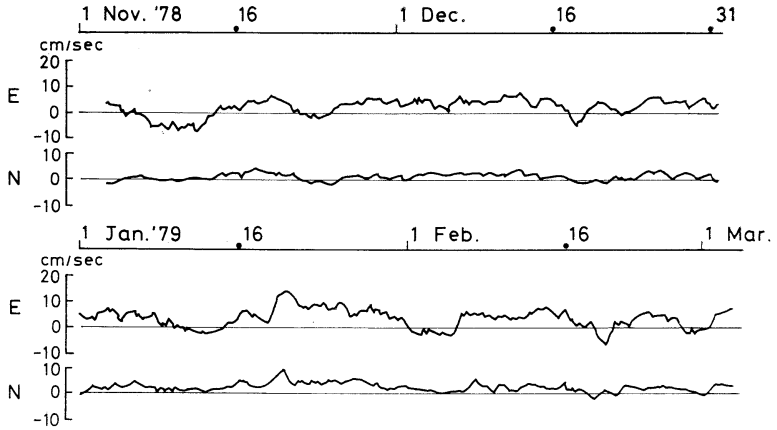

Fig. 18. Current speeds averaged over 25 hours at 700 m.

elevations at Ishigaki Harbor are shown in Table 2 (NAKANO, 1940). The order of the amplitude of tidal constituents for all elements is equal to the order of the amplitude of the surface elevations at Ishigaki Harbor. The phase difference of the M_2 constituent of current between 300 and 700 m is about 90°; it is inferred that the tidal structure in this area is somewhat baroclinic.

The tidal ellipses of the four major tidal constituents at 300 and 700 m are shown in Figs. 15 and 16. The tidal ellipses of the M_2 constituents are dominant at 300 and 700 m. The tidal ellipses of the four major tidal constituents are somewhat flat due to the influence of the coast line. The rotation of the tidal constituent is clockwise.

7. Long-term variations of the current

Figs. 17 and 18 show the current speeds averaged over 25 hours of the eastward and northward components at 300 and 700 m. The time series at 300 m shows larger fluctuations of several days to a month but seldom has the minus values for either component. The time series denotes smaller fluctuations at 700 m than at 300 m of several days to a month.

8. Summary

Current measurements by using self-recording current meters were carried out from early November 1978 to early March 1979. The location of the measurements is to the northwest of Iriomote Island, between Taiwan and Yaeyama Islands, and is about 1,000 m deep. Current meters, Bergen Model-4, were set at 300 and 700 m. The current direction and speed, temperature, salinity and pressure were measured. A mooring line was buoyed upward from a weight on the sea bottom by a buoy cluster which consists of nine floats. Two timed releases were attached to the lower end of the line. A back-up rope on the ground was attached above the release and was moored by a mushroom anchor. The back-up rope could be retrieved with a grapnel if two releases acted before the preset time or if we could not arrive at the mooring position because of prohibitive sea conditions.

The power spectral analysis of current variations shows that the most prominent peak corresponds to the semidiurnal period and the secondary peak corresponds to the diurnal. The shallow-water tides (M_3, M_4) were clearly found in the spectra at a depth of 700 m. Almost no inertial period (29 hours at 24°N) was found in these spectra. The harmonic analysis of the four major tidal constituents, M_2, S_2, K_1 and O_1, shows the magnitude of the amplitude of each constituent to be in the order of $M_2 > S_2 > K_1 > O_1$, just as the order of the amplitude of surface elevations. The phase difference of the M_2 constituent between 300 and 700 m was about 90°, suggesting that the tidal structure in this area was baroclinic.

The current speeds averaged over 25 hours

varied greatly from 0 to 1.5 knots with period from several days to a month.

Acknowledgements

The authors wish to express their hearty thanks to the staff of the Science and Technology Agency. They are very grateful to Professor M. IWASHITA, Tokai University, for his encouragement, to the staff members of Institute of Oceanic Research and Development, Tokai University, for their assistance, to the crew of the research and training ship Tokai Daigaku Maru II, and to the staff of Ship Management Section, Tokai University, for the mooring operation.

References

CHU, T.Y. (1976): Study of the Kuroshio Current between Taiwan and Ishigakijima. Acta Oceanographica Taiwanica, **6**, 1-24.

NAKANO, M. (1940): Chosekigaku (in Japanese). Kokon-shoten, Tokyo. 528 pp.

UDA, M. (1934): Oceanographic condition of Japan Sea and its adjacent area (in Japanese). Bull. Japan. Soc. Sci. Fish., **7**, 91-151.

西表島近海における流動測定

淵　秀隆，佐藤孫七，稲葉栄生，川畑広紀，辻　康子

要旨: KER（黒潮開発利用）の一環として，本邦八重山列島西表島近海の水深 1000 m 地点で，昭和53年度の寒候期に4ケ月間自記測流を実施した。測流層は 300 m および 700 m の2層で，水中ブイにより海底から立ち上げた係留線の 300 m および 700 m 層にアンデラ流速計を取り付けた。回収の為に係留線下端の錘りの直上に時限式の切離装置を取り付け，またアンカー付の長いグランドロープを切離装置の上方から海底に伸ばした。

測得流のスペクトルは，300 m および 700 m の両層とも半日周潮が顕著に卓越し，1日周潮がこれにつぎ，慣性周期は卓越しない。潮流の卓越順序は $M_2 > S_2 > K_1 > O_1$ で，潮位の卓越順序と一致する。M_2 分潮の 300 m 層と 700 m 層との位相差は約 90° であり，当海域における潮汐構造がバロクリニックな現象であると推論される。25時間移動平均流は，2～3日から1カ月位の周期をもって 0～1.5ノットの間を大きく変動している。

La mer 20: 21-28, 1982
Société franco-japonaise d'océanographie, Tokyo

Distribution and Seasonal Changes of Metals in Water of Lake Biwa*

Akira KURATA**

Abstract: Distribution and seasonal changes in concentration of 13 kinds of metals were investigated at the designated stations in the north and south basins of Lake Biwa. Concentrations of the dissolved form of Li, Sr, Cr, Mn, Fe, Co, Ni, Cu, Zn, Mo, Cd, Sb and Pb ranged 0.03-0.19, 20.9-49.2, 0.26-2.84, 1.6-21.5, 17.1-133.2, 0.98-3.13, 3.5-17.6, 2.2-19.3, 3.2-31.9, 0.4-6.0, 0.21-1.02, 1.8-9.8 and 1.0-8.3 μg/l, respectively, in water during the investigation period (April 1978-March 1979). In Zn and Mn, concentrations of the particulate form were higher than those of the dissolved form. In Cu and Co, on the contrary, concentrations of the particulate form were lower than those of the dissolved form. In the south basin, seasonal changes in the concentrations of 11 kinds of metals had a similar pattern at each station. In the north basin, concentrations of a few kinds of metals were rather higher at the easterly stations than at the westerly stations. Such a distribution pattern suggested a prominent supply of these metals by river water at the east coast of the lake.

1. Introduction

In recent years, heavy metal pollution has proceeded extensively in Lake Biwa, especially in the south basin of the lake. Therefore, the heavy metal contents in bottom sediments and in different kinds of invertebrates and vertebrates have been investigated by many researchers in the coastal region of the lake. However, the concentrations of metals, except for major elements, in water of Lake Biwa and their seasonal changes have not yet been made clear owing to very low level of the concentration of each metal, in spite of the quality of water being a matter of great significance for 13 million people in Kyoto, Osaka and Kobe districts receiving water supply from this lake.

In the present study, an attempt was made to make clear the concentration and distribution of 13 kinds of metals in water of Lake Biwa.

* Received June 3, 1981
This work was financially supported by the Environment Conservation Bureau of Prefectural Government of Shiga.

** Department of Fisheries, Faculty of Agriculture, Kyoto University, Kitashirakawa-Oiwake-cho, Sakyo-ku, Kyoto, 606 Japan

2. Materials and methods

(*1*) *Collection of water samples*

Samples of lake water were collected with a Van Dorn water sampler during the period from April 1978 to March 1979 at the designated stations in the south and north (main) basins of Lake Biwa (Fig. 1A and B). In both basins, sampling was made once a week during spring and generally once a month during the other seasons.

(*2*) *Determination of metals*

Water samples collected were immediately brought to the laboratory, filtered through Whatman GF/C glass fiber filters and adjusted the pH value to 1-2 with conc. HNO_3. Before the filtration, the glass fiber filters were soaked in 3N-HNO_3 for 24 hr and washed thoroughly with deionized distilled water in order to avoid the contamination by trace metals contained in the filters. After this pretreatment, the filters were always checked for the metal concentrations. Since the concentrations of many kinds of metals in water samples were very low, a large volume of water (4-6 *l*) was sampled and concentrated to approximately 10 m*l* by evaporation under reduced pressure at 60°C for the determination of dissolved metals. Separately, metals contained in the particulates collected on the glass fiber

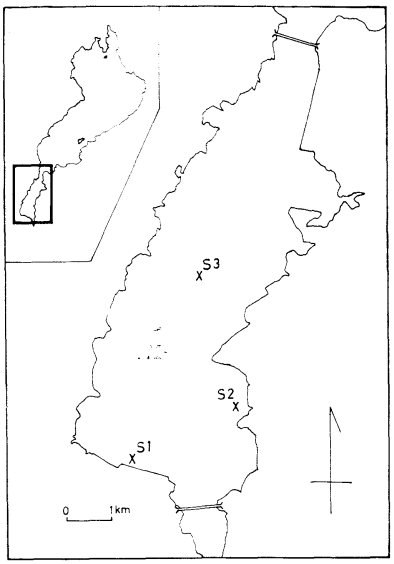

Fig. 1A. Location of the stations in the south basin of Lake Biwa.

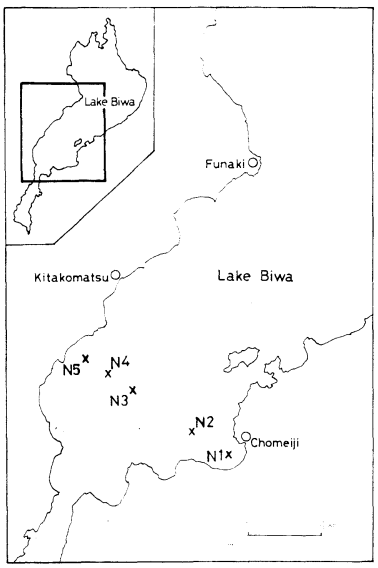

Fig. 1B. Location of the stations in the north basin of Lake Biwa.

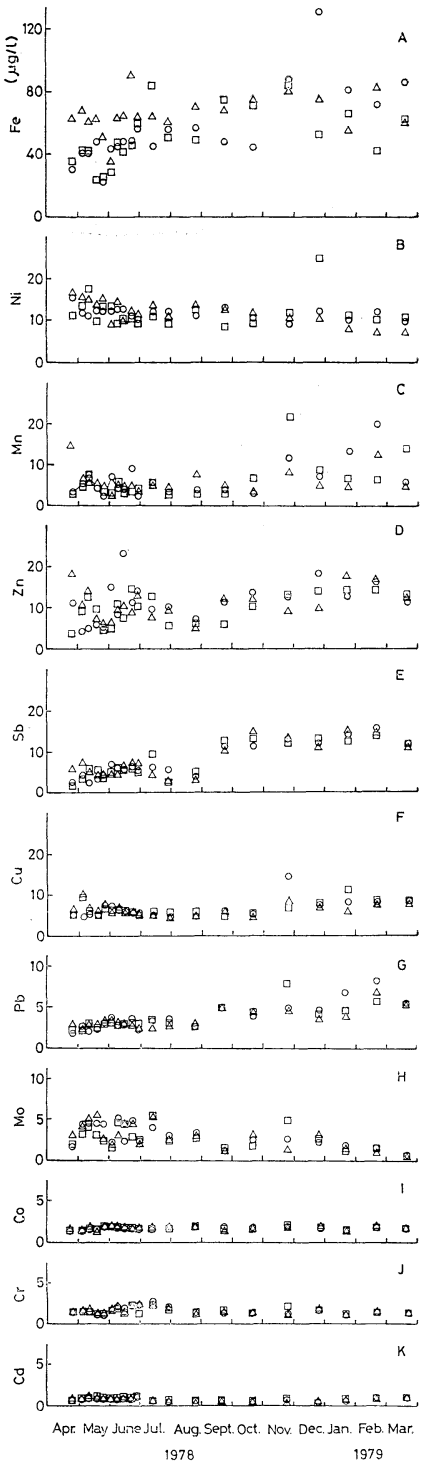

Fig. 2. Seasonal changes in the concentrations ($\mu g/l$) of dissolved metals in water at Stations S1 (○), S2 (△) and S3 (□) in the south basin of Lake Biwa from April 1978 to March 1979.

Table 1. Concentrations ($\mu g/l$) of particulate metals in water in the south basin of Lake Biwa. Average values in parentheses.

	Stn. S1	Stn. S2	Stn. S3
Fe	64.4 -132.5 (105.4)	10.3 -199.1 (122.5)	36.8 -192.3 (123.5)
Zn	18.6 - 80.3 (34.6)	5.2 -136.1 (54.0)	11.8 -203.9 (54.4)
Ni	0.1 - 2.9 (1.2)	0.03- 2.5 (1.3)	0.3 - 2.4 (1.1)
Cu	0.6 - 3.8 (1.7)	0.2 - 4.2 (1.6)	0.3 - 2.6 (1.4)
Mn	13.6 - 38.4 (25.1)	9.1 - 73.9 (39.3)	5.0 - 39.3 (23.0)
Pb	1.3 - 5.2 (3.2)	0.4 - 5.2 (2.9)	1.8 - 6.9 (3.6)
Mo	0.9 - 5.3 (3.7)	0.4 - 6.0 (4.1)	1.4 - 7.4 (3.8)
Co	0.01- 0.72 (0.24)	0.01- 0.48 (0.14)	0.01- 1.01 (0.29)
Cr	0.74- 2.30 (1.14)	0.06- 2.52 (0.92)	0.75- 2.86 (1.43)
Cd	0.07- 0.68 (0.23)	0.04- 0.79 (0.30)	0.01- 5.54 (0.69)
Sb	0.57- 5.70 (2.78)	0.42- 5.46 (2.66)	0.57- 4.98 (3.06)

Table 2. Concentrations ($\mu g/l$) of dissolved metals in water in the north basin of Lake Biwa. Average values in parentheses

	Stn. N1	Stn. N2	Stn. N3	Stn. N5
Fe	24.5 -57.8 (44.5)	17.2 -62.5 (39.5)	17.1 -46.5 (33.6)	23.9 -56.9 (34.3)
Zn	6.3 -18.5 (10.7)	6.1 -18.8 (9.9)	6.2 -25.6 (11.6)	4.9 -11.8 (8.8)
Ni	6.0 -11.8 (8.8)	6.1 - 9.9 (7.9)	4.1 -12.8 (8.1)	5.1 -10.3 (7.6)
Cu	3.8 - 6.4 (4.9)	2.2 - 7.1 (4.6)	2.7 - 6.7 (4.3)	2.9 - 5.1 (4.5)
Mn	1.2 -11.4 (4.5)	0.6 - 5.7 (2.6)	0.9 - 3.5 (1.7)	0.8 - 3.5 (1.7)
Pb	1.2 - 3.7 (2.5)	1.0 - 4.4 (2.6)	1.3 - 3.6 (2.1)	0.8 - 3.1 (2.2)
Mo	1.6 - 5.3 (2.9)	1.3 - 4.2 (2.5)	0.4 - 3.8 (1.7)	0.9 - 2.6 (1.3)
Co	1.11- 1.96 (1.49)	1.19- 2.51 (1.64)	0.98- 2.63 (1.66)	1.04- 1.96 (1.52)
Cr	0.51- 1.44 (1.01)	0.62- 1.51 (1.13)	0.26- 1.34 (0.85)	0.51- 1.52 (1.01)
Cd	0.20- 0.78 (0.43)	0.15- 0.48 (0.27)	0.22- 0.49 (0.36)	0.15- 0.69 (0.41)

Table 3. Concentrations ($\mu g/l$) of particulate metals in water in the north basin of Lake Biwa. Average values in parentheses.

	Stn. N1	Stn. N2	Stn. N3	Stn. N5
Fe	60.5 -162.5 (91.2)	25.6 -65.8 (49.7)	14.5 -53.7 (28.8)	13.3 -52.9 (23.5)
Zn	26.0 - 80.2 (47.0)	17.3 -92.2 (45.5)	21.1 -83.6 (33.9)	12.3 -48.3 (30.9)
Ni	1.5 - 10.6 (4.5)	1.8 -10.5 (3.9)	0.9 - 5.2 (3.2)	1.5 - 6.9 (3.8)
Cu	0.5 - 2.3 (1.4)	0.5 - 1.6 (0.9)	0.4 - 1.3 (0.7)	0.4 - 2.4 (0.8)
Mn	6.2 - 19.9 (10.7)	1.9 - 8.1 (5.6)	3.0 - 8.3 (4.6)	2.6 - 8.2 (4.0)
Pb	0.9 - 4.2 (1.9)	0.8 - 2.8 (1.7)	0.8 - 2.2 (1.5)	0.5 - 5.4 (1.8)
Mo	2.0 - 7.0 (3.4)	1.3 - 4.3 (2.3)	0.5 - 3.4 (1.7)	0.5 - 3.4 (1.4)
Co	ND- 0.95 (0.41)	0.09- 0.81 (0.40)	0.13- 0.73 (0.31)	0.12- 0.71 (0.30)
Cr	0.45- 3.73 (1.34)	0.45- 1.92 (1.14)	0.40- 1.44 (0.86)	0.23- 1.69 (0.80)
Cd	0.05- 0.94 (0.21)	0.04- 1.02 (0.25)	0.03- 0.16 (0.09)	0.04- 0.39 (0.23)

filters were extracted with 3N-HNO_3. The concentrations of Li, Sr, Cr, Mn, Fe, Co, Ni, Cu, Zn, Mo, Cd, Sb and Pb were determined by the atomic absorption spectrophotometric method described in the previous paper (KURATA, 1974).

3. Results and discussion

Patterns of seasonal changes in the concentrations of 11 kinds of metals are shown in Fig. 2. During 12 months from April 1978 to March 1979, the concentrations of Fe, Ni, Mn, Cu, Zn, Sb, Pb, Mo, Co, Cr and Cd ranged 22.0–133.2, 6.5–26.8, 2.1–21.5, 3.8–19.3, 3.4–18.0, 1.8–15.8, 1.5–8.3, 0.3–6.0, 1.07–2.11, 0.53–2.84 and 0.21–1.02 $\mu g/l$, respectively. According to reports on the bottom sediments of the south basin of the lake, the maximum content of Ni, Mn, Cu, Zn, Pb, Cr and Cd amounted to 70, 2450, 116, 736, 306, 74.6 and 26 $\mu g/g$ dry matter, respectively (ITASAKA *et al.*, 1971, TATEKAWA *et al.*, 1971, NAKAMURA *et al.*, 1972, NAKAMURA *et al.*, 1974, KOBAYASHI *et al.*, 1975). However, the concentrations of metals in water have not been made clear in these reports. The concentrations of Fe, Mn and Zn fluctuated considerably during the investigation period. On the other hand, the concentrations of Ni, Cu, Co, Cr and Cd remain little changed excepting a few cases for Ni and Cu. The concentrations of Fe, Mn, Sb and Pb were fairly low from spring to summer and fairly high from autumn to winter. Generally, seasonal changes in the concentrations of all kinds of metals at each station showed similar patterns.

Concentrations of the particulate metals in water at each station from April to August of 1978 are shown in Table 1. It was thought that the greater part of particulates must be composed of phytoplankton. At these stations, in average, 105.4–123.5 μg of Fe, 34.6–54.4 μg of Zn, 23.0–39.3 μg of Mn, 2.9–3.6 μg of Pb, 1.1–1.3 μg of Ni, 1.4–1.7 μg of Cu, 3.7–4.1 μg of Mo, 0.14–0.29 μg of Co, 0.92–1.43 μg of Cr,

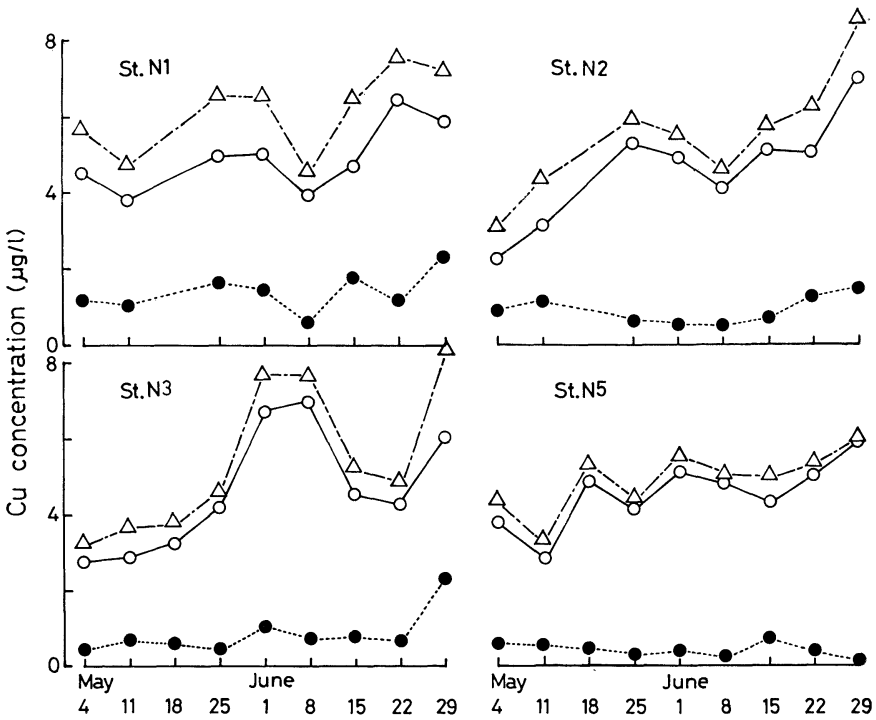

Fig. 3. Variations of dissolved (○), particulate (●) and total (△) Cu concentrations in the north basin of Lake Biwa from May to June 1978.

0.23–0.69 μg of Cd and 2.66–3.06 μg of Sb were contained in 1 *l* of water as particulate form. The particulate form of Fe, Zn and Mn was at higher level than the dissolved form of these metals. This corresponds to rather low level of dissolved form of those metals during the growing season of phytoplankton as shown in Fig. 2. On the contrary, the particulate form of Ni, Cu, Co and Sb was at rather lower level than the dissolved form. In the cases of Pb, Mo, Cr and Cd, there is little difference between the particulate and the dissolved form.

Concentrations of 10 kinds of metals in water at each station in the north basin of the lake are shown in Table 2. The concentrations of Fe, Zn, Ni, Cu, Mn, Pb, Mo, Co, Cr and Cd ranged 17.1–62.5, 4.9–25.6, 4.1–12.8, 2.2–7.1, 0.6–11.4, 0.8–4.4, 0.4–5.3, 0.98–2.63, 0.26–1.52 and 0.15–0.78 μg/*l*, respectively. The concentrations of Fe, Ni, Mn, Pb and Mo were nearly half compared with those in the south basin of the lake. However, the concentrations of Zn, Cu, Co, Cr and Cd were almost the same as those in the south basin of the lake. From these data, it may be supposed that the discharge of some kinds of metals from the rivers flowing into the south basin of the lake was more intense than in the north basin.

The concentrations of particulate metals in water at each station in the north basin of the lake are shown in Table 3. The concentrations of Fe and Mn in this form were considerably lower than those in the south basin. It may be that the amounts of these metals taken up by phytoplankton were affected by lower level of these metals in water of the north basin than in water of the south basin. However, the concentrations of particulate form of other metals were almost the same as those in the south basin.

Relative proportion of the dissolved and the particulate forms in the total amount differed with metals in the north basin as well as in the south basin. In the cases of Zn and Mn, particulate form occupied greater part of the total amount irrespective of seasons and sampling stations. On the contrary, in the cases of Cu

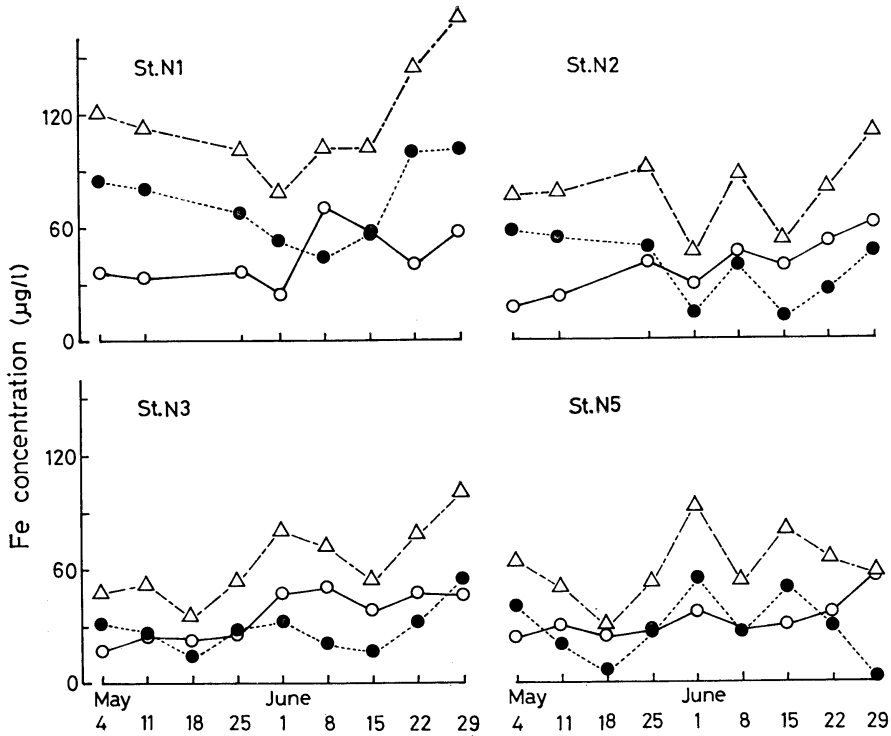

Fig. 4. Variations of dissolved (○), particulate (●) and total (△) Fe concentrations in water in the north basin of Lake Biwa from May to June 1978.

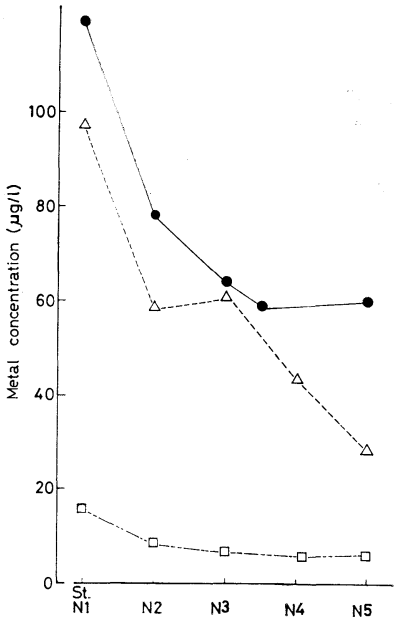

Fig. 5A. Averaged values of the total (dissolved +particulate) concentration of metals in water in the north basin of Lake Biwa during the investigation period. ●, Fe; △, Zn; □, Mn.

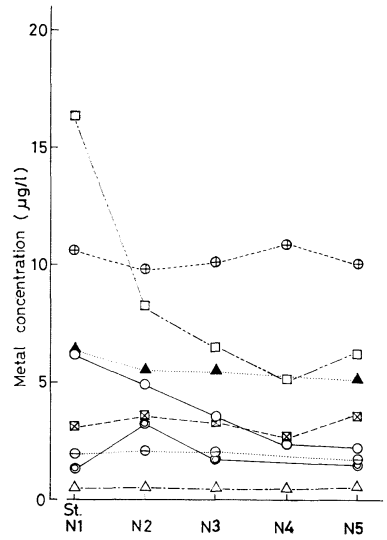

Fig. 5B. Averaged values of the total (dissolved +particulate) concentration of metals in water in the north basin of Lake Biwa during the investigation period. □, Mn; ⊕, Ni; ▲, Cu; ○, Mo; ⊠, Pb; ◎, Cr; ⊖, Co; △, Cd.

Table 4. Concentrations ($\mu g/l$) of dissolved metals in water of Lake Biwa from April 1978 to March 1979.

	Range	Average
Fe	17.1 -133.2	43.6
Sr	20.9 - 49.2	15.8
Zn	3.2 - 31.9	9.9
Ni	3.5 - 17.6	10.1
Sb	1.8 - 9.8	4.7
Mn	1.6 - 21.5	3.4
Cu	2.2 - 19.3	5.4
Pb	1.0 - 8.3	2.6
Mo	0.4 - 6.0	2.6
Co	0.98- 3.13	1.63
Cr	0.26- 2.84	1.33
Li	0.03- 0.19	0.70
Cd	0.21- 1.02	0.42

and Co, dissolved form occupied the major portion of the total. While, in the cases of Fe and Mo, the proportion of both forms varied significantly in accordance with the sampling days. It is supposed that the fraction of particulate form in the total reflected the requirement of these metals by phytoplankton during the investigation period. Variations in dissolved, particulate, and total Cu and Fe at each station in the north basin of the lake during the growing season of phytoplankton are shown in Figs. 3 and 4.

Distribution of the averaged values of total amount of each metal in water at each station from the east to the west in the north basin of the lake during the investigation period is shown in Figs. 5A and B. The concentrations of Fe, Zn and Mn showed a marked trend to be higher at the easterly stations than at the westerly stations. However, the concentrations of other metals had not such a striking tendency at these stations. It is suggested from such distribution pattern that the major elements must be mainly supplied through the rivers in the east coast of the lake from paddy fields, domestic waste water and discharge of many factories.

Variation in the concentrations of 13 kinds of metals in water of the lake during the investigation period is summarized in Table 4. Comparing with the concentrations of metals in other

lakes, the concentrations of Cu, Zn and Cr in water of Lake Biwa were less than one-fifth of those in Lake Orta (GERLETTI and PROVINI, 1978). The concentrations of Mn, Cu and Zn in water of Lake Biwa were at the same level as those of Lake Michigan (ROSSMANN and CALLENDER, 1969), although the concentration of only Ni in the former lake was slightly higher than that in the latter.

Acknowledgements

The author is grateful to the staff of Shiga Prefectural Institute of Public Health and Environmental Science and to the members of Otsu Hydrobiological Station of Kyoto University for their kind assistance in sampling program during the investigation period.

References

GERLETTI, M. and A. PROVINI (1978): Effect of nitrification in Orta Lake. Prog. Wat. Tech., **10**, 839-851.

ITASAKA, O., Y. OKUMURA, T. HORI, K. HASHIMOTO and Y. OHYAMA (1971): On the water quality of Lake Biwa, the Seta River and some rivers in Otsu City and the heavy metal content of bottom matters of Lake Biwa. Report Limnol. Lab. Shiga Univ., **11**, 1-12 (in Japanese).

KOBAYASHI, J., F. MORI, S. MURAMOTO, S. NAKASHIMA, H. TERAOKA and S. HORIE (1975): Distribution of arsenic, cadmium, lead, zinc, copper and manganese contained in the bottom sediment of Lake Biwa. Jap. J. Limnol., **36**, 6-15 (in Japanese).

KURATA, A. (1974): Cobalt content in the shallow sea sediments. J. Oceanogr. Soc. Jap., **30**, 199-202.

NAKAMURA, M., S. NAKANO and M. TATEKAWA (1972): Studies on the sediments deposited in Lake Biwa (VI). The distribution of rare metal elements in the surface sediments of bottom of Lake Biwa. Report Limnol. Lab. Shiga Univ., **12**, 60-82 (in Japanese).

NAKAMURA, M., S. NAKANO and M. TATEKAWA (1974): Studies on the sediments deposited in Lake Biwa (IX). On the heavy metal elements contained in the bottom sediments in the southern part (Nan-ko) of Lake Biwa (Prediction). Report Limnol. Lab. Shiga Univ., **14**, 59-66 (in Japanese).

ROSSMANN, R. and E. CALLENDER (1969): Geochemistry of Lake Michigan manganese nodules. Symp. 12th Conf. Great Lakes Res., 306-316.

TATEKAWA, M., M. NAKAMURA and M. KANEZAKI (1971): Studies on the sediments deposited in Lake Biwa (V). The distribution of heavy metal elements in the surface sediments of bottom of Lake Biwa (Prediction). Mem. Fac. Educ. Shiga Univ., Nat. Sci., **21**, 88-112 (in Japanese).

びわ湖湖水中における金属の分布と季節変動

倉田　亮

要旨: びわ湖南湖および北湖の湖水中における13種類の金属の濃度と季節変動を調べた。溶存態の各金属の濃度は Li, Sr, Cr, Mn, Fe, Co, Ni, Cu, Zn, Mo, Cd, Sb および Pb がそれぞれ，0.03～0.19，20.9～49.2，0.26～2.84，1.6～21.5，17.1～133.2，0.98～3.13，3.5～17.6，2.2～19.3，3.2～31.9，0.4～6.0，0.21～1.02，1.8～9.8 および 1.0～8.3 $\mu g/l$ の範囲内で変動がみられ，また，粒子態の各金属濃度は，Cr. Mn, Fe, Co, Ni, Cu, Zn, Mo, Cd, Sb および Pb がそれぞれ，0.06～3.73，1.9～73.9，10.3～199.1，ND～1.01，0.03～10.6，0.2～4.2，5.2～203.9，0.4～7.4，0.01～5.54，0.42～5.70 および 0.4～6.9 $\mu g/1$ の範囲内で変動した。南湖においては，溶存態の Fe および Mn の濃度が春から夏にかけてとくに低く，秋から冬にかけて高かったが，その他の金属の濃度については著しい季節的な変動がみられなかった。一方，北湖においては，溶存態の Zn, Cu, Co, Cr および Cd の濃度は南湖とほぼ同じ程度であったが，Fe, Ni, Mn, Pb および Mo の濃度が 1/2 程度の値であった。各金属には粒子態として存在する割合の高いものと溶存態の割合が高いものとがあり，Zn および Mn は前者に，Cu および Co は後者に属し，Fe や Mo は定点や時期によって大きく両者の割合が変動した。北湖における Fe, Zn, Mn などの濃度の高い金属の全量（溶存態＋粒子態）の分布は概して東岸寄りで高く，西岸寄りで低い傾向がみられ，東岸の各河川からの流入による影響がかなり大きいものと推測された。

La mer 20: 29-36, 1982
Société franco-japonaise d'océanographie, Tokyo

数値実験からみた1883クラカトア津波*

中　村　重　久**

1883 Krakatoa Tsunami in a Scope of Numerical Experiment*

Shigehisa NAKAMURA**

Abstract: 1883 Krakatoa tsunami around the Sunda Strait was studied by using a simple numerical model for finite difference method. The author tried to find properties of tsunami front, arrival time and tsunami height on the basis of the numerical experiment. Estimated value of the wave energy trapped in the Sunda Strait was about 54% of initial increase of an equivalent potential energy at the tsunami source area being due to a vertical displacement of the water surface. This result seems to be successfully applicable to a tsunami in a strait or channel of similar dimension, e.g. the Kii Channel in Japan.

1. 緒　言

1883年8月27日の大噴火によってクラカトア火山の大部分が吹きとばされ，その影響は全世界に及んだ。この噴火に関連して，たとえば，英国のRoyal Societyは報告書をまとめ(SYMONS, 1888)，最近でも資料の収集・整理が行なわれている(ANON., 1980)。SYMONS (1888) の報告書の第3章には，Capt. W.J.L. Whartonが，噴火による津波についての資料とその解析について述べている。また，この噴火に関連した研究は多数にのぼっている(PIGEAUD, 1968; DEPT. PERTANIAN, 1968; KUSUMADINATA, 1979; PERPUSTAKAAN, 1938; JUDD, 1899)。これらの多くは，噴火や地震についての記述に詳しく，津波については簡単に述べられているか，ほとんどふれられていないかである。SYMONS (1888) の報告書 (p. 142) によれば，クラカトア大噴火によって，西オーストラリア海岸の Cossack (20°41′S, 117°11′E) では，27日午後4時に異常潮位がみとめられ，それはおよそ5フィートであった。また，Geraldton では，27日午後8時，突然6フィートも潮が引いた。さらにまた，津波の年表 (SOLOVIEV and GAO, 1974) によれば，クラカトア大噴火による津波は遠く南米太平洋岸に達し，0.5～1 m の高さであったという。

NAKAMURA (1979, 1980) は，インドネシアにおける津波の発生および来襲についての統計的研究を通して，その予測を検討したが，そこでは，海底地震による津波のみを解析の対象として，火山噴火による津波はその発生機構が異なるものと考え除外した。この津波の評価には，火山学的問題，地震学的問題も関連しているものと考えられる。ちなみに，SOLOVIEV and GAO (1974) によれば，1883年8月27日10時02分，クラカトア大噴火により津波が発生し，その高さは，スマトラ島南岸で 4 m，ジャワ島西岸および南岸で 2-2.5 m であった。

また別に，TERADA (1923) の述べるところによれば，“クラカトア爆発時の波は，インド洋はもとより，太平洋，大西洋までもひろがった。理論 ($v=\sqrt{g(h+a)}$; 水深 h，津波の高さ a に対する波の速さ) からみた到達時刻より実際の到達時刻

* 1981年10月9日受理 Received October 9, 1981
** 京都大学防災研究所附属白浜海象観測所
〒649-23 和歌山県西牟婁郡白浜町堅田畑崎
Shirahama Oceanographic Observatory, Disaster Prevention Research Institute, Kyoto University, Katada-Hatasaki, Shirahama, Wakayama, 649-23 Japan

はおそい。このときの長波の周期は，ジャワ島とスマトラ島との間の海峡に生ずる副振動の周期であった”。

火山活動や山崩れにともなう津波に関する研究としては，相田 (1975, 1977) が九州の島原半島，眉山について行なった数値実験の例がある。このような津波をどのように評価するかについては，いろいろの立場からの議論があるものと考えられる。ここでは，火山噴火による津波を，海底地震による津波と同様な考え方と取り扱いができるとして，中村 (1981 a, b) が用いたと同じ有限差分法により，1883年のクラカトア火山の大噴火にともなう津波の数値実験を試みた。この数値実験の結果にもとづき，津波の伝播特性，津波の高さ，津波の到達時刻のほか，波源域の等価水面変位高の評価にもとづき，スンダ海峡内に trap された津波のエネルギーの推定をした。スンダ海峡がわが国の紀伊水道と同程度のスケールであることを考えあわせると，ここで得られた結果は，津波の予測と関連して示唆にとんでいるものと考えられる。

2. 数値実験の対象領域

1883 クラカトア津波は，インド洋のみならず太平洋や大西洋にも伝わったといわれている。ちなみに，スンダ海峡から南極環海を経て南米の太平洋岸と大西洋岸に至る可能な径路は Fig. 1 の P および A と考えられる。径路 P を津波がとって南米太平洋岸で 0.5-1 m の津波の高さが観測されるということは力学的に考えられうることであろうか。径路Mおよび Z はそれぞれスンダ海峡から子午線および緯度内に沿って南極大陸およびアフリカ大陸に至るが，当時，そこで津波が観測された可能性があったとしても，そこに目撃者あるいは住民がいなければ，記録としては残らないことになる。このように，1883 クラカトラ津波は全地球的スケールでとらえるべきであるかもしれないが，ここでは，Fig. 2 のように，スンダ海峡周辺部のスマトラ東部およびジャワ西部の海域を対象として考える。数値実験にあたっては，3-11°S と 102-108°E とで囲まれる海域を対象とし，緯度経度それぞれ 1/5° 間隔の格子網をとることにした。この海域の水深分布は，海上保安庁水路部発行の海図より内挿によって求めた。この海域のうち，ジャワ海の水深はジャカルタ付近の 50 m が最大であった。また，スンダ海溝の最大水深は 5,600 m

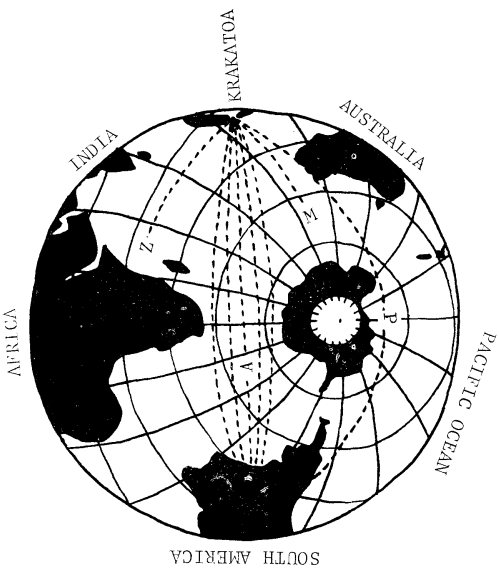

Fig. 1. Wave rays of 1883 Krakatoa tsunami.

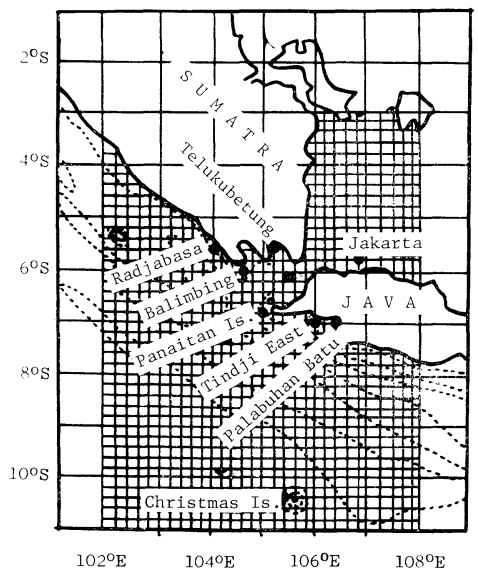

Fig. 2. Schematic grid spacing diagram for a numerical experiment of 1883 Krakatoa tsunami.

ととった。以上の水深条件と格子間隔とから，時間ステップとして，$\Delta t=0.01913$ hr をとった。

3. 波源域

波源域としては，Fig. 2 に示すように，スンダ海峡のクラカトア火山に対応する格子点4点によって構成される方形水域（およそ 44×44 km^2）を考えた。波源域の初期水面条件を特徴づけるものとして，これまでの数値計算（中村，1981a, b, c）と同様にして，水面の変位高 W とその持続時間 T とを考えた。この W と T との組合せにより等価波源の条件づけをすることにしよう。実際の数値計算の都合上，水面の変位高を $W=0.1$ m とした。また，その持続時間として $T=100$, 200, 400, 800 sec ととる場合を中心にして検討する。対象水域内のすべての格子点（陸地を除く）で津波の計算値は得られるが，ここでは，そのうち，スマトラ島についてはスンダ海峡内の Telukubetung，インド洋沿岸の Balimbing および Radjabasa，ジャワ島については北岸の Jakarta，南岸の Tindji East および Palabuhan Batu，そして，クリスマス島に最も近いと考えられる格子点（Fig. 2 参照）における計算結果を示すことにした。

4. 津波のフロントの伝播

津波の原因となったクラカトア火山の噴火過程を，どのようにして数値実験でとりいれるかについてはなお不明な点が多い。ここでは等価なパラメーターとして，波源域での水面変位高 W とその持続時間 T を考える。実際の W の値はかなり大きかったにちがいないが，さしあたって，数値計算の都合上，$W=0.1$ m とした場合に着目し，その基本特性をとらえることとする。いま，W の 0.001 倍の変位を津波のフロントとみると，クラカトア津波のフロントの伝播図は Fig. 3 のようになる。数値計算モデルでのフロントの伝播は持続時間 T には関係がない。Fig. 3 では，0.2時間後にはフロントはインド洋へ出ている。さらに1時間後にはインド洋上のフロントはクリスマス島を通過しており，その時，ジャワ海のフロントは，まだ波源域からそれほど距ってはいない。インド洋上のフロントは，あたかも点波源から同心円状に広がる波，コーシー・ポアソン波によく似ている。

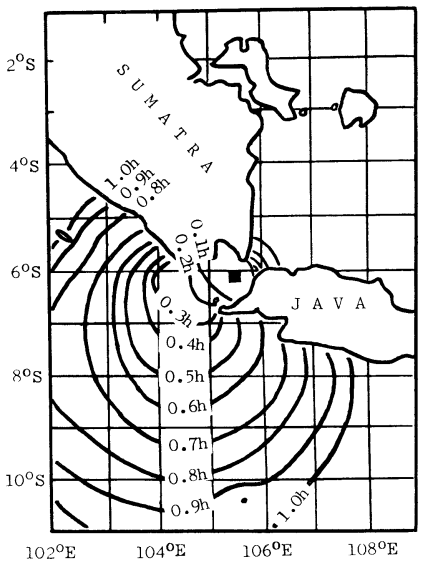

Fig. 3. Propagation of tsunami front.

5. 海岸付近の津波

計算で得られた津波の波型は，たとえば，$W=0.1$ m の条件で，$T=100$ sec では Fig. 4(a) のようになる。$T=200$ sec および 400 sec では Fig. 4(b) および (c) のようになる。ここで対象とした範囲の持続時間では，各点での一定時刻の水面変位高は，持続時間 T に比例しているとみてよい。この傾向は，中村（1981a）による1977スンバワ津波の数値実験の例や，大阪湾・紀伊水道の津波の数値モデル（中村，1981b）の例などにおいて認められた傾向と同じである。この詳細については後に述べる。ただ，T が十分小さければ，発生した波はコーシー・ポアソン波に近いものとなり，T が十分大きければボアに近いものになるであろう。しかし，クラカトア火山の噴火を考えるかぎり，T がある程度以上大きい値は現実的ではない。かりに，任意の T についての数値計算ができたとしても，それが実際の現象として可能かどうかについて十分吟味する必要がある。また，スンダ海峡周辺の海岸線や海底地形は複雑であるから，波は反射，屈折，回折をくりかえし，波形は変形して，

さらに複雑なものとなる。もし，計算対象水域で津波を含む検潮記録があれば，計算波形がもっともらしいかどうかを確かめることができるはずである。

TERADA (1923) は，このクラカトア津波の周期は，スンダ海峡内に生ずる副振動の周期と同じであると述べているが，Fig. 4 の計算結果からみるかぎり，このような副振動の周期が卓越しているとみられるのは，スンダ海峡に面した海岸のみにおいてであると考えられる。スンダ海峡のスマトラ島とジャワ島との間で生じた横振動を考えると，大まかにみて，平均水深 $h=90$ m，海峡の幅 $L=60$ km で，単節振動の Merian の周期として $T_M=1.1$ h が得られる。この T_M の値は Telukubetung における計算波形の特徴をうまく説明しているものと考えられる。

また，Fig. 4 をみると，スンダ海峡の波源域に近い点，Telukubetung，Radjabasa，Balimbing，Panaitan Island では，いずれも第1波はひき波で始まっている。波源域の初期条件として，水面

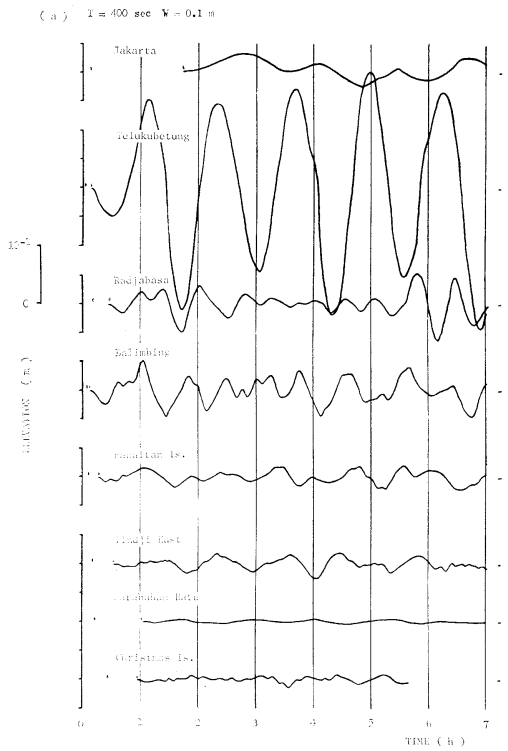

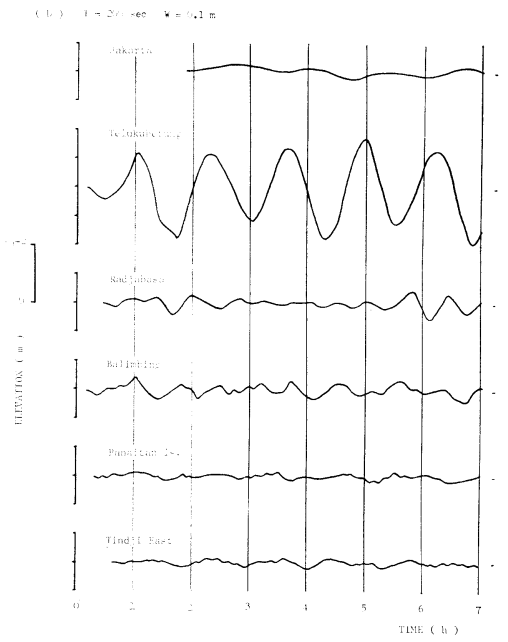

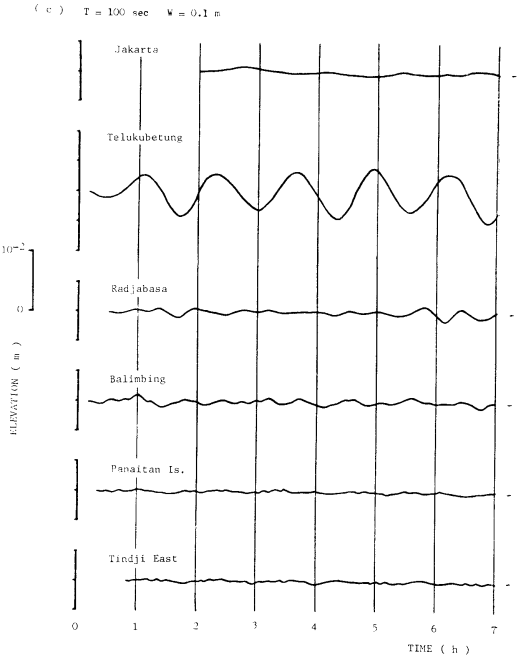

Fig. 4. Computed mareograms of 1883 Krakatoa tsunami model for $W=0.1$ m. (a) $T=400$ sec, (b) $T=200$ sec and (c) $T=100$ sec.

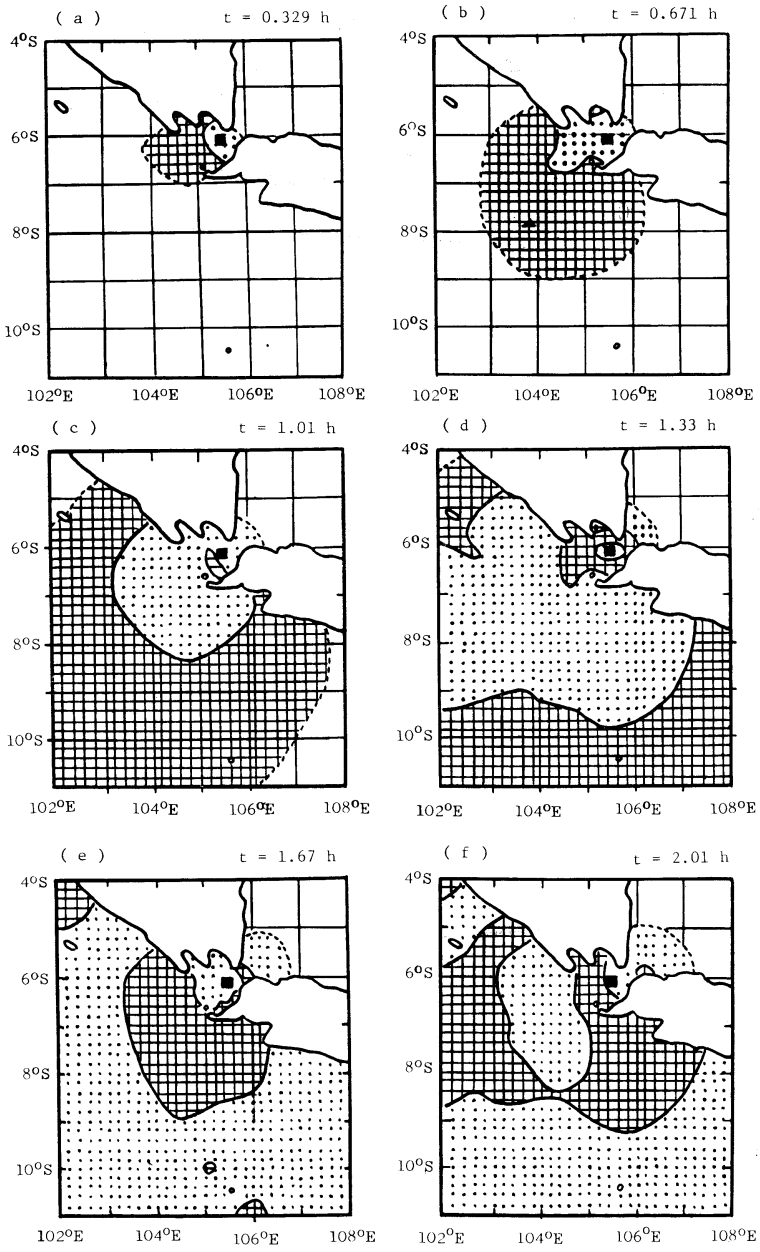

Fig. 5. Time-stepping wave patterns of 1883 Krakatoa tsunami model. (a) t=0.329 h, (b) t=0.671 h, (c) t=1.01 h, (d) t=1.33 h, (e) t=1.67 h and (f) t=2.01 h.

の上昇を考えた場合，スンダ海峡のような限られた狭い水域での急速な変動現象では，このことは妥当なものと考えられる。これは，たとえば，たらいの中の水の中央部が急にもりあがると，その周囲の水位は低下することになることに対応するものと考えられるからである。この様な機構については別に力学的に検討する必要がある。

6. クラカトア火山からの津波のひろがり

波源域で与えられた擾乱は，時の経過とともに周囲の水域へとひろがっていく。数値計算の結果にもとづいて，$W=0.1$ m，$T=100$ sec の例について，Fig. 5 (a)-(f) にその様子を示した。津波のフロント（破線）は W の 0.001 倍の変位をとり，その後の変位ゼロを実線で示した。2つの実線あるいは破線と実線とで囲まれる海域について，水面擾乱が初期静水面より上になった水域を格子模様とし，下になった水域を黒点模様とした。すなわち，Fig. 5(a) からみると，波源域近くは水面が初期水位より低下しており，スンダ海峡のインド洋側では初期水位より高い水位があらわれていることを示している。このような水面擾乱は時々刻々とその位置をかえていくが，これを Fig. 4(a) とあわせてみると，インド洋上での水面擾乱はスンダ海峡内に比較して非常に小さいことがわかる。Fig. 5(a)-(f) からみても明らかなように，水面擾乱のパターンは必ずしも単純ではない。

7. 津波の到達時刻

津波の到達時刻について，中村 (1981a, b) は，計算によって得られる時刻 P と，検潮記録など実測において到達時刻と判断される時刻 Q とが考えられるとしている。ここで，クラカトア火山からの津波についての計算例を Table 1 に示す。ただし，波源域で $W=0.1$ m，$T=100$ sec とした。この表からみてもわかるように，スンダ海峡の外では，Q_5 や Q_4 をたとえ計算で求めることができても，検潮記録から求めることは難しい。ただし，Q_4 は，たとえば，1977 スンバワ津波に対する西オーストラリア海岸の Q_3 のように重力長波の伝播速度 $\sqrt{gh}$ によって伝播したとしても説明できる程度の到達時刻になることがある。これは，TERADA (1923) が述べている傾向と一致している。さらに，また，MUNK (1980) が 1951 年核爆発実験による津波について述べているところとも傾向が定性的によく一致している。

8. 津波の高さ

数値計算の結果から津波の高さを求めると，波

Table 1. Arrival time of Krakatoa model tsunami.

Station	P (arrival of disturbance)		Q	
	displacement (m)	time (h)	Q_5 (h) [$\|H\|=10^{-5}$m]	Q_4 (h) [$\|H\|=10^{-4}$m]
Jakarta	1.32×10^{-22}	0.134	1.57	1.97
Telukubetung	-7.23×10^{-7}	0.0574	0.0957	0.153
Radjabasa	-8.09×10^{-2}	0.172	0.383	0.498
Balimbing	-1.03×10^{-6}	0.0766	~0.11	~0.15
Panaitan Island	-6.89×10^{-11}	0.0957	~0.22	~0.3
Tinji East	-1.06×10^{-7}	0.172	~0.53	~1.1
Christmas Island	9.14×10^{-47}	0.421	~0.88	~1.8

Table 2. Height of Krakatoa model tsunami.

Station	Duration time			
	$T=100$ sec	$T=200$ sec	$T=400$ sec	$T=800$ sec
Jakarta	6.52×10^{-4} (m)	1.30×10^{-3} (m)	3.25×10^{-3} (m)	7.08×10^{-3} (m)
Telukubetung	4.06×10^{-3}	8.11×10^{-3}	2.01×10^{-3}	4.27×10^{-2}
Radjabasa	1.16×10^{-3}	2.32×10^{-3}	5.68×10^{-3}	1.14×10^{-2}
Balimbing	1.10×10^{-3}	2.17×10^{-3}	5.17×10^{-3}	9.28×10^{-3}
Panaitan Island	4.87×10^{-4}	9.52×10^{-4}	2.14×10^{-3}	3.40×10^{-3}
Tindji East	3.86×10^{-4}	7.81×10^{-4}	1.92×10^{-3}	3.23×10^{-3}
Christmas Island	2.32×10^{-4}	4.44×10^{-4}	9.85×10^{-4}	1.89×10^{-3}

源域の水面変位と津波の高さとの関係を知ることができる。いま，波源域の水面変位を $W=0.1$ m とし，その持続時間を $T=100, 200, 400, 800$ sec とすると，各点での13時間にわたる計算波から得られた津波の高さは Table 2 のようになる。

SOLOVIEV and GAO (1974) の津波年表によれば，スンダ海峡内では，津波の高さは 30 m であり，スマトラ南岸で 4 m，ジャワ島北岸および南岸で 2-2.5 m となっている。これに対応するような津波の高さの分布は，Table 2 では $T=100$ sec の例と考えられる，波源域での水面変位が大きく，しかも，周辺海域の海岸線や海底地形が複雑であれば，非線型効果も顕著と考えられる。ひとつの目安として，Table 2 で $T=100$ sec の場合の津波の高さを7,000倍すると，スンダ海峡内の Telukubetung で 28 m，スマトラ南岸の Balimbing で 7.7 m，ジャワ島南岸の Panaitan Island で ～3.5 m となっていて，大体の傾向は上述の津波年表の数字と一致する。このような考え方が妥当であるとすると，波源域での W の値としては，700 m 程度を等価水面変位として考えるのが適当であるということになる。なお，Table 2 に示した津波の高さは，津波の第1波の峯高とは必らずしも同じではない。

中村 (1981a) は，津波の数値モデルで格子間隔を $\Delta x=\Delta y=4{,}540$ m とし，検潮記録と計算波形を比較してその再現性を検討した。しかし，1977スンバワ津波のインドネシア海岸での挙動について，20 km の格子網による数値実験（中村，1981b）では，その再現性には，若干不確かなところも残っていた。ちなみに，中村 (1981c) が 1977 スンバワ津波の西オーストラリア海岸における挙動を検討した例では，格子間隔を 27.5 km としたところ，津波の波形を3時間移動平均によって平滑化したものが数値計算で再現されていることがわかった。これらの例をみると，1883クラカトア津波が果してどれだけ再現できているかを注意深く吟味する必要がある。ただ，TERADA (1923) のスンダ海峡における副振動に関する記述は，数値計算の結果からみて，Telukubetung の水位変動の特性とよく対応しているようにみえる。これによって津波が再現されたとみるかぎりにおいて，ここに示した数値計算の結果は意味のあるものと考えることができる。

9. 津波のエネルギー

クラカトア火山の噴火によって，波源域で700 m 相当の水面変位があったと考えたとしても，Fig. 4 によれば，Telukubetung では $0.007\times7{,}000=49$ m 相当の水位変動（周期約 1.1 hr）がおよそ7時間ほとんど減衰することなく持続している。ここで問題なのは，実際に，このように複雑な海岸線と海底地形をもった水域で，長時間にわたり，かなり大振幅の水位変動のエネルギーが逸散しないとはふつう考え難いことである。かりに，地形の影響や海底摩擦によるエネルギー損失が小さかったとしても，エネルギーの他の一部はインド洋へ，そしてごく小部分はジャワ海へ逸散していくものと考えるのが，従来の考え方にのっとり計算結果を解釈する立場である。かくして，Fig. 4 の例からみて，スンダ海峡内の津波エネルギーは，スンダ海峡内の水位変動維持に効果的に使われ，急速に減衰する様子はうかがわれない。

波源域で水面変位 $\Delta h=700$ m に対するポテンシアル・エネルギーの単位水面積あたりの変化分を

$$E_p'=\rho g\Delta h\sim7{,}000\ \mathrm{N\cdot m}$$

と考える。このとき，波源域の全ポテンシアル・エネルギーの変化分を，格子点4点に相当する面積 S に対して考えると，

$$E_p=(\rho g\Delta h)\,S.$$

ところで，$S=4\times(22)^2\ \mathrm{km}^2$ であるから，

$$E_p=1.355\times10^{13}\ \mathrm{N\cdot m}.$$

一方，Telukubetung の波高から，スンダ海峡内の水位変動のエネルギーを大まかに推定する。波高を $H=25$ m とすると，単位面積あたり

$$E_T'=\frac{1}{8}\rho gH^2.$$

このとき，スンダ海峡内の格子点25点相当の水面積を考え，水位変動に関与した全エネルギーを求めると，

$$E_T=\left(\frac{1}{8}\rho g H^2\right)A.$$

ここに，$A\sim 25\times(22)^2\ \mathrm{km}^2$ であるから，

$$E_T\sim 7.33\times 10^{12}\ \mathrm{N\cdot m}.$$

これから，スンダ海峡から外海へ出た津波エネルギーは

$$\Delta E=E_p-E_T\sim 6.22\times 10^{12}\ \mathrm{N\cdot m}$$

となり，波源域のエネルギーの約 46％が外海へ，約 54％が海峡にという割合になる。Fig. 4 によれば，Telukubetung で第1波の峯高は，すでに，後続波の峯高とほぼ同じであり，波高もあまり変化していないことからみて，このエネルギー分配過程は，津波発生後 1-2 時間という比較的短時間の間にみられたものと考えられる。

このような推定の妥当性を検証するには，さらに，別の資料にもとづく考察が必要であろう。ここでは，津波の全地球的なひろがりについて検討するところまでにはいたらなかった。

謝　辞

本研究着手のきっかけは，前オーストラリア科学産業庁国土管理部 (CSIRO Divison of Land Resources Management) 上級研究員 Mr. BARRY CARBON との討議によるところが大きい。また，文献資料の利用には，京大防災研海岸災害部門土屋義人教授，白浜海象観測所吉岡洋助手のほか，CSIRO Div. LRM の Mr. RAY PERRY (Chief), Dr. HENRY ALLISON (上級研究員), Mr. GRAEM OLSEN, 西オーストラリア大学土木工学科教授 RICHARD SILVESTER, 地理学科図書館長 Mr. VIV FORBES, 地質学科講師 Mr. HUGH A. DOYLE, インドネシア国立科学研究所科学資料センター情報部 Dr. UTARI BUDIHARJO の協力と好意とを得た。なお，数値計算にあたっては，京大大型計算機センター FACOM M-200，京大防災研災害科学資料センター FACOM M-140，および京大化研中央計算機室 FACOM M-160AD を利用した。

文　献

相田　勇 (1975): 1792 年島原眉山崩壊に伴った津波の数値実験．地震，**28**，449-460.

相田　勇 (1977): 山崩れによる津波．海洋科学，**9**，103-110.

ANONYMOUS (1980): The eruption of Krakatoa. Science, **207**, 1336 (excerpted from Science, Vol. 12 (old series), 9 Nov. 1888, pp. 217-219).

DEPARTEMEN PERTANIAN (1968): Bibliografi Mengenai Krakatau, Seri Bibliografi: No. 9, Lembagan Perpustakaan Biologi dan Pertanian "Bibliotheca Bogoriensis", pp. 1-22.

JUDD, J. W. (1889): The earlier eruption of Krakatoa. Nature, 15 Aug. 1889, pp. 365-366.

KUSUMADINATA, K. (Ed.) (1979): Data Dasar Gunungapi Indonesia (Catalogue of references on Indonesian volcanoes with eruptions in historical time), Departemen Pertanbangan dan Energi, Direktrat Vulkanologi, pp. 112-124 (in Indonesian).

MUNK, W. (1980): Affairs of the sea. Ann. Rev. Earth Planet. Sci., **8**, 1-16.

NAKAMURA, S. (1979): On statistics of tsunamis in Indonesia. Southeast Asian Studies, **16**(4), 664-674.

NAKAMURA, S. (1980): A note on statistics of historical tsunamis in Southeast Asia. Proc. Internat. Conf. Engineer. Protect. Nat. Disast., Asian Inst. Technol., Bangkok, pp. 883-894.

中村重久 (1981a): 数値実験からみた 1977 スンバワ津波．La mer, **19**, 30-37.

中村重久 (1981b): 大阪湾・紀伊水道の津波の数値モデル．La mer, **19**, 105-110.

中村重久 (1981c): 西オーストラリア海岸の長周期波について．第28回海岸工学講演会論文集，土木学会，pp. 44-48.

PERPUSTAKAAN (Kon. Bataviaaisch Gesootschap van K. en W.) (1938): Laftar buku-buku, tentang ilmu bumi dan ilmu bangsa, Kepulauan Indonesia, Djakarta, pp. 91-104.

PIGEAUD, T. G. Th. (1968): Literature of Java; Catalogue raisonné of Javanese manuscripts in the library of Reiden and other public collections in the Netherlands, the Hague, Martinus Nijhoff, II, pp. 308-853.

SOLOVIEV, S.L. and Ch. N. GAO (1974): Catalogue of Tsunamis in Western Coast of the Pacific Ocean. Acad. Sci. USSR, Izdat. Nauk. 310 pp. (in Russian).

SYMONS, S.J. (1888): The eruption of Krakatoa and subsequent phenomena. Report, Krakatau Committee, Royal Society, London. 376 pp.

TERADA, T. (1923): Umi no Buturigaku (Physics of the Sea), 3rd ed. Rigaku (Science), Vol. 2. Nippon-no Romaji-Sya, Tokyo. 125 pp.

La mer 20: 37-40, 1982
Société franco-japonaise d'océanographie, Tokyo

The First JECSS (Japan and East China Seas Study) Workshop (Introduction)*

Takashi ICHIYE**

1. Background

It seems ironic that political and economical interest is focused on marginal or adjacent seas of the world as manifested in declaration of 200 miles economic zones by many countries when oceanographers start in the seventies to cooperate in big projects for studying deep sea oceanography of the North Atlantic and Pacific Oceans, and the Southern Ocean. Although the marginal seas are considered important economically, the natural processes predominant there are more complicated than those in deep oceans because of effects of coastal and bottom boundaries, thus usually they have shunned these areas except for a special process such as coastal upwelling.

We cannot emphasize too much that oceanographers should cooperate for studying the marginal seas in the eighties for several reasons. One reason is purely scientific. Nearshore and shallow water processes are predominantly nonlinear but provide major roles in energy dissipation (and probably supply, too) for the oceanic circulation. Other reasons are economical and political. Aside from obvious political and economical importance of these seas (such as transportation and resource exploitation), oceanographers will encounter difficulties in going out far into the interior of the ocean owing to fuel shortage and in doing field study of these seas by political interference of some coastal countries.

There are great differences in geographic features among the marginal seas of the world oceans, although the gross features of ocean circulation have similarity at least between the North Pacific and North Atlantic Oceans. The adjacent seas of the western North Pacific Ocean have a broad continental shelf as those of the western North Atlantic Ocean but the similarity seems to end there. Particularly the former seas are more complicated not only in the coastlines but also in hydrographic characteristics, in a sense that the Japan Sea interrupts the continental shelf of the South and East China Seas with a deep semi-enclosed basin and the two large rivers, the Yantze (Changiang) and the Yellow (Huanghe), transport enormous amounts of sediments together with fresh water into the East China Sea and Bohai Bay, respectively. There are many interesting and important oceanographic problems to be studied in these areas. Since before the WW II many oceanographic activities were taken in the East China Sea and the Japan Sea mainly by Japan. Since early sixties these activities have been accelerated particularly by Japan Meteorological Agency, Fisheries Agency and Hydrographic Department of Japan and also have been augmentented by researchers from USSR, Korea and China, partly through CSK (Cooperative Study of Kuroshiro) Program, though China was not an official member of the program.

The hydrographic data mainly with Nansen bottle casts, collected by the Japanese oceanographers in these areas surpass those in any other parts of the world oceans in their frequency and density, according to assessment by Dr. Choule SONU of TEKMARINE in California. Only lacking is the synthetic analysis of these data for general understanding of ocean dynamics and for identification of specific processes. After completion of scientific assessment of these data, there will emerge need of new cooperative programs for collecting additional data or for carrying out new experiments. Two examples may be cited. Routine hydrographic cruises of the East China Sea were extensively carried out seasonally and sometimes bimonthly by Nagasaki

* Received December 22, 1981
** Department of Oceanography, Texas A & M University, College Station, TX 77843, USA

Marine Observatory and Fisheries Agency of Japan since early fifties (KOIZUMI, 1964), but there is no work which correlates the discharge from the Yantze to water mass distribution and circulation there. There was a good review by MORIYASU (1972) on the Tsushima Current, but it is still unknown why this current branches from the Kuroshio at the Tsushima Straits with a wide shelf less than 100 m in depth interrupting the two currents west of Kyushu. A paper by MINATO and KIMURA (1980) is the first step for rational explanation of generation of the current as a result of pressure difference between the Tsugaru and Tsushima Straits due to the wind-driven oceanic circulation. More elaboration of this mechanism will be discussed including the non-linear effects in a paper to be included in the proceedings which will combine papers published in this journal.

2. Development of the Workshop

I was marginally interested in the Tsushima Current as described by comparing it with the Loop Current in the Gulf of Mexico in my paper published in an obscure journal almost twenty years ago (ICHIYE, 1962). Early last year SONU called my attention to his study on the Tsushima Straits hydrography by combining satellite infrared (IR) images with extensive hydrographic data collected by the Japanese oceanographers. He also mentioned that Dr. Dennis CONLON of Louisiana State University just finished his dissertation on hydrography of the Tsugaru Straits. He suggested that I could contact the Japanese physical oceanographers who might be interested in cooperative study of hydrography of these straits, the Japan Sea and the East China Sea. I attended UNESCO-WESTPAC Workshop on Coastal Transport of Pollutants convened by Prof. Toshiyuki HIRANO, Ocean Research Institute, University of Tokyo in late March last year. I stayed in Japan for several days for interviewing some physical oceanographers for potential participation in a joint cooperative study of the two seas. This activity was facilitated by my attendance of the national meeting in April of Oceanographical Society of Japan in Tokyo. During summer and fall of last year I had extensive discussion with SONU and CONLON who moved to the Office of Naval Research in Mississippi as well as with Dr. Ya HSUEH who was at the National Science Foundation at the time and Prof. Kenzo TAKANO of Tsukuba University about convening some preliminary meeting in Japan next year on physical oceanography of the two seas. At first, one faculty member of Tokai University, Shimizu, appeared to be interested in such a meeting. Thus in late October I sent a preliminary letter of a symposium to be convened in the spring, 1981 possibly at that campus on dynamics of marginal seas of the western North Pacific Ocean to potential participants of Japan, U.S., People's Republic of China, Korea and USSR. I received more than twenty favorable answers to my letter before the end of November.

Next few months I was engaged in writing to various foundations in Japan for possible funding for the proposed symposium as well as in finding a suitable acronym for the symposium, which is said to be most important for promotion of any project, according to some top scientists in the U.S. It turned out that all the foundations contacted by me could not support the meeting for one reason or other. Further in late January the faculty member of Tokai University informed me of unavailability of the campus for the meeting because of some objection from the administration. Fortunately TAKANO saved the day by offering his university as a meeting place and his service as a co-convener. Moreover, he contacted Prof. Koji HIDAKA for financial support for the meeting through HIDAKA Foundation which graciously provided the sum of ¥400,000 in spite of an extremely short notice of application. As for the acronym, the first choice was MIDAS/JESUS (Multinational Investigation of Dynamics of Adjacent Seas/Japan and East China Seas Unified Study). However, this was too long and besides as several friends of mine pointed out, combination of names related to objects of material and spiritual worship might offend some people, though there is no intention for my part for allusion. Thus finally JECSS was chosen and the official invitation letter for the workshop was sent to potential participants around the middle of February.

The letter stated that the workshop would be held at Tsukuba University from 1 June to 4 June. Its three main objectives are: (1) identification of hydrographic data sources and descriptive reviews of the circulation in the two seas; (2) critical appraisal of mathematical and experimental models on dynamics of the area, and (3) discussion on planning of future study including field experiments with ships, drifters, mooring systems and satellites.

3. The Meeting

All participants from U.S., Korea and P.R.C. and some from Japan were housed in guest houses of Tsukuba University. The program of the workshop is listed in the appendix. Twenty-four papers were presented at the meeting. Contents of papers presented will be summarized with names and affiliation of participants elsewhere (ICHIYE, 1982). Therefore, here only synthetic discussion on the last day of the program is described based mainly on notes taken by Noel PLUTCHAK of Interstate Electronics, Anaheim, California.

First, the Steering Committee for JECSS was established in order to facilitate cooperative study of the two seas, exchange information of progress and organize and publicize the future meetings. Each country elected a representative for the committee except Japan which may elect two representatives. Voice votes confirmed TAKANO as one representative of Japan, Dr. Kuh KIM of Seoul National University as the representative for Korea and ICHIYE as the chairman and representative for the U.S. Mr. Y. YUAN of Second Institute of Oceanology, P.R.C. wished to postpone about the representative until consulting with his colleagues.

The main items decided in this session are: (1) the second workshop will be held in April 1983 in Japan; (2) some participants will make effort for IOC to recognize and support JECSS as one of its working group, (3) invitation will be sent to Taiwan before next meeting, (4) cooperative calibration and standardization of data will be developed, (5) cooperative field surveys, for instance in the East China Sea for Fall of 1981 and Spring of 1982 between U.S. and Korea will be scheduled and the plan and the results will be disseminated through the steering committee, (6) the First JECSS Workshop papers will be published in "*La mer*", (7) the fields covered will be limited tentatively for physical aspects including chemical and geological oceanography, (8) meeting review may be published in Japan in JOSJ and in the U.S. in EOS of AGU.

It is noted that personal contacts among the participants were superb during and after sessions each day because of relatively small numbers of participants, closely located lodging and meeting places and excellent assistance by staff and students of the university. Such contacts were further enhanced at the get-together evening of the first day on campus and the barbeque party at Mt. Tsukuba in the afternoon of the last day, both of which were organized expertly by TAKANO and his group. (I also acknowledge travel expenses of two trips to Japan were partially provided by the Office of Naval Research.)

References

ICHIYE, T. (1962): Circulation and water mass distribution in the Gulf of Mexico. Geofisica Internacional, Mexico, **2**, 46-76.

ICHIYE, T. (1982): The First JECSS Workshop at Tsukuba University, Ibaraki, Japan. Scientific Bulletin, ONR Tokyo (to be published).

KOIZUMI, M. (1964): On the standard deviation of the surface temperature of the East China Sea (in Japanese). *Studies of Oceanography* (Prof. Hidaka's Commemorative Volume), Univ. of Tokyo Press, p. 140-144.

MINATO, S. and R. KIMURA (1980): Volume transport of the western boundary current penetrating into a marginal sea. J. Oceanog. Soc. Japan, **36**, 185-195.

MORIYASU, S. (1972): The Tsushima Current. *Kuroshio, Its Physical Aspects* (Edited by H. STOMMEL and K. YOSHIDA), Univ. of Tokyo Press, p. 353-370.

Monday 1 June, 1981

Morning — Chairman—C. SONU

Opening remark ····· ICHIYE, T. (U.S.A.)

1. Estimation of the Kuroshio mass transport flowing out from the East China Sea to the North Pacific ····· NISHIZAWA, J., E. KAMIHARA, R. KUMABE and M. MIYAZAKI (Japan)
2. Seasonal and year-to-year variability of the Tsushima-Tsugaru Warm Current System with its possible cause ····· TOBA, Y., K. TOMIZAWA, Y. KURASAWA and K. HANAWA (Japan)
3. Formation of water masses in the Japan Sea ····· KIM, K. (Korea)

Afternoon — Chairman—Y. HSUEH

4. On the large internal fluctuations observed on the Korean coast of the Japan Sea ····· SEUNG, Y. H. (Korea)
5. Sediment transport in the East China Sea ····· MILLIMAN, J. (U.S.A.)
6. Current transport of sediments ····· KOLPACK, R. L. (U.S.A.)
7. Distribution of metallic elements in sea water in the East China Sea ····· SUGIMURA, Y. and Y. SUZUKI (Japan)

Tuesday 2 June

Morning — Chairman—Y. TOBA

8. Water properties and currents around the Jeju Island in June, 1981 ····· KIM, K. (Korea)
9. Dynamics of flow in the region of Tsugaru Straits ··· CONLON, D. (U.S.A.) (Presented by SONU, C.)
10. Three dimensional numerical model of the coastal circulation ····· HSUEH, Y. (U.S.A.)
11. Calculation of three dimensional ocean current by exact solution—finite element method ····· YUAN, Y., J. SU and J. ZHAO (P.R.C.)
12. A single layer model of the continental shelf circulation in the East China Sea ····· YUAN, Y. and K. HE (P.R.C.)

Afternoon — Chairman—M. ENDOH

13. A tidal model of the Yellow Sea and the East China Sea ····· CHOI, B. (Korea)
14. Note on currents driven by a steady uniform wind stress on the Yellow Sea and the East China Sea ····· CHOI, B. (Korea)
15. Numerical modeling of the Japan Sea ····· YOON, J. (Japan)

Wednesday 3 June

Morning — Chairman—M. TAKEMATSU

16. Inventory of oceanographic data for sea straits around the Japan Sea ····· SONU, C. (U.S.A.)
17. Precaution for environmental monitoring in the shallow sea ····· PLUTCHAK, N. (U.S.A.)
18. Satellite observations of surface circulation patterns of the Japan Sea, East China Sea and Yellow Sea: Fall, winter and spring seasons ····· HUH, O. (U.S.A.)
19. A case study of SST and water quality mapping by spacecraft data ····· MUNEYAMA, K., Y. SASAKI, I. ASANUMA and T. EMURA (Japan)

Afternoon — Chairman—O. K. HUH

20. On the short-term variability of the Kuroshio and Tsushima Current ····· TAKEMATSU, M. (Japan)
21. Hydrographic study of the East China Sea ··· BEARDSLEY, R. (U.S.A.) (Presented by MILLIMAN, D.)
22. On the internal wave resonance in the Yellow Sea ····· AN, H. S. (Korea)
23. A review of sea conditions in the Japan Sea ····· SHUTO, K. (Japan)
24. The continental shelf waves in the eastern coast of Korea ····· CHUNG, J. K. (Korea)

Thursday 4 June

Morning — Chairman—K. KIM

Synthetic discussion ····· all the participants

Closing remark ····· HSUEH, Y. (U.S.A.)

La mer 20: 41-51, 1982
Société franco-japonaise d'océanographie, Tokyo

Seasonal and Year-to-Year Variability of the Tsushima-Tsugaru Warm Current System with its Possible Cause*

Yoshiaki TOBA**, Kazumi TOMIZAWA**,
Yoshikazu KURASAWA** and Kimio HANAWA**

Abstract: The current transport entering the Japan Sea may be regarded as balancing with that flowing out the Sea, in a time scale longer than the seasonal. Regarding the Tsushima Current and the Tsugaru Current as the main warm current system passing through the Japan Sea, the most plausible image of the variability and its possible cause are presented, by synthesizing accumulated observational data. The average seasonal variation of the volume transport is characterized by the minimum in February through May, and the maximum in August through September. The annual average is $2.0\times10^6 m^3 s^{-1}$ with a range of variation of $1.6\times10^6 m^3 s^{-1}$. It is inferred that the current system is driven and controlled by the difference of sea level or ΔD, between the shallow East China Sea where the temperature variation by air-sea interaction is large, and the cold sea area east of Tsugaru which is the westmost part of the subarctic gyre. The following formula is proposed for both the seasonal and the year-to-year variability: $V(10^6 m^3 s^{-1})=2.0+0.1\Delta H$ (cm), where V is the volume transport of the current system, ΔH is the deviation from the average of the sea level difference between the East China Sea and the area east of Tsugaru, and for seasonal variability, there is a delay of phase of one to two months in the volume transport.

1. Introduction

The Tsushima Warm Current flows from the East China Sea into the Japan Sea, forming the major inflowing transport to the Japan Sea. This water flows through the southern half of the Japan Sea to the northeast, converging off Akita and Aomori Prefectures to flow to the north along the Japanese coast. The majority of the transport then flows out through the Tsugaru Strait into the Pacific Ocean as the Tsugaru Warm Current, while a minor portion flows further north and becomes the Soya Warm Current emerging through the Soya Strait to the Sea of Okhotsk. A part of the transport flowing north in the eastern part of the Japan Sea presumably flows back southwards through the western part as the cold Liman Current. This part of the transport may be considered as the circulating transport within the Japan Sea. This is the primary description of the current system through the Japan Sea (cf. Fig. 1).

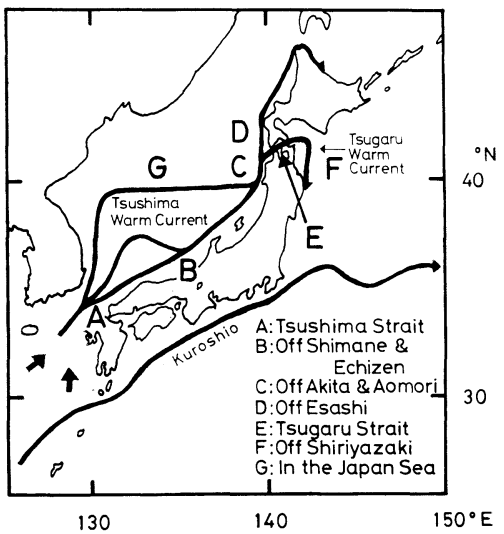

Fig. 1. Schematic picture of the warm current system through the Japan Sea. Key letters A through G stand for location of stations in Table 1.

* Received August 31, 1981
Presented at the First JECSS Workshop, June 1981 (cf. La mer, **20**: 37-40, 1982).
** Geophysical Institute, Faculty of Science, Tohoku University, Sendai, 980 Japan

The Tsushima Current was regarded as one branch of the Kuroshio departing from the main current to the southwest of Kyushu. However, it has been recognized that the Tsushima Current is sometimes an ill-defined, diffuse flow of water from the East China Sea through the entire Tsushima Strait* (e.g. AKAMATSU, 1977). The mechanism of the variability has not yet been shown.

Also, it seems generally accepted that the Tsugaru Current is caused by the difference in sea level between the Japan Sea and the North Pacific Ocean (e.g. HATA, 1973), but the cause of the sea level difference had not hitherto been elucidated.

Recently, MINATO and KIMURA (1980) have treated the western boundary current penetrating into a marginal sea by use of a linear, steady and barotropic model, and have shown that about 2 % of the volume transport of the Kuroshio will penetrate into the Japan Sea. This may give a rough interpretation for the currents through the Japan Sea. However, seasonal variation of the Tsushima Current is not necessarily parallel to that of the Kuroshio, and also the Tsushima Current is not an exact branch of the Kuroshio, but consists of a mixture of the Kuroshio water and the water of the East China Sea. Further, the Tsugaru Strait is not located along the western boundary current, but at the west end region of the subarctic gyre.

In this report, we have approached the problem with a working hypothesis that the variability of the warm currents penetrating the Japan Sea is determined by the sea level difference between the shallow East China Sea, where the sea level variation is large owing to the effective air-sea interactions, and the cold and deep subarctic region to the east of Tsugaru Strait, where features of the air-sea interaction and the sea level variation are different from the East China Sea. It will be reported below that we have reached a conclusion supporting this hypothesis.

* In this report the term "Tsushima Strait" is used, for simplicity, as a combination of the Korea Strait and the Tsushima Strait in the narrow sense.

According to the tidal records, the maximum range of sea level fluctuation within one month in the Japan Sea is 20 cm, which can be converted to an average excess inflowing or outflowing transport of $0.1 \times 10^6 m^3 s^{-1}$. The evaporation and the precipitation correspond to the same order of magnitude or smaller. These values are one order of magnitude smaller than the average transport of the Tsushima Current. Consequently, insofar as we consider the variability of the transport penetrating the Japan Sea in a time scale longer than one month, or at least a seasonal time scale, it may be assumed that the inflowing and the outflowing transports vary synchronously. This assumption seems to have been postulated by MORIYASU (1972) in his review paper on the Tsushima Current.

The transport of the Soya Current is not large (AOTA, 1975), and according to HATA (1962) and KIMURA (1978) 70 to 90 % of the transport of the Tsushima Current flows out as the Tsugaru Current. Consequently, we treat the main element of the transport passing through the Japan Sea in a time scale longer than the seasonal variability as the Tsushima-Tsugaru Warm Current System.

2. Variability of the current system synthesized from the past data

Table 1 shows a list of studies up to the present which estimate the velocity and/or the volume transport of currents in relation to the Japan Sea. Fig. 2 shows the synthetic time series from these studies.

In order to draw a representative variability of the current system, we choose the volume transport off Akita and Aomori Prefectures, where the warm current flows to the north with a narrow cross section, and where the assumption that the barotropic component is small may be used. This assumption has actually data supported by CONLON (1981). Data obtained by direct current measurement are still scanty, so we should rely on accumulated hydrographic data at the present stage. Fig. 3 is an ensemble of the estimated seasonal variability from various sources. Data points from the present study show the geostrophic transport, which has been estimated with a

Table 1. List of studies up to the present on variability of the warm currents in the Japan Sea. For location of observation sections, see Fig. 1.

Author	Location of section	Period of estimation	Reference level	Remark*
SUDA (1938)	A	1932-35	bottom	V
HIDAKA & SUZUKI (1950)	A (Korea Strait)	1926-41	Two Layers (zero speed in lower layer)	V
KUSUNOKI & KASHIMA (1951)	C, D	1921-47		V
MIYAZAKI (1952)	A, C, D	1935-40(A) 1931-40, 48, 50(C, D)	bottom(A) deeper than 400db (C, D)	T
SUGIURA (1958)	F			V, T
YASUI & HATA (1960)	C, F	1957-58(C) 1950-58(F)	400db	T
HATA (1962)	C, D	1947-59	400db	T
YI (1966)	A		125db	V, T
AKAMATSU (1974)	C	1966-73	300db	T
AOTA (1975)	D			V, T (from tide records)
KIMURA (1978)	B, G		500db	T
AKABANE (1979) AKABANE *et al.* (1979)	C, F	1966-79	300db(C) 400db(F)	T
Present Study	A, C, D, E	1966-76(A) 1964-80(C)	bottom(A, E) 300db(C, D)	T

* V, velocity; T, volume transport.

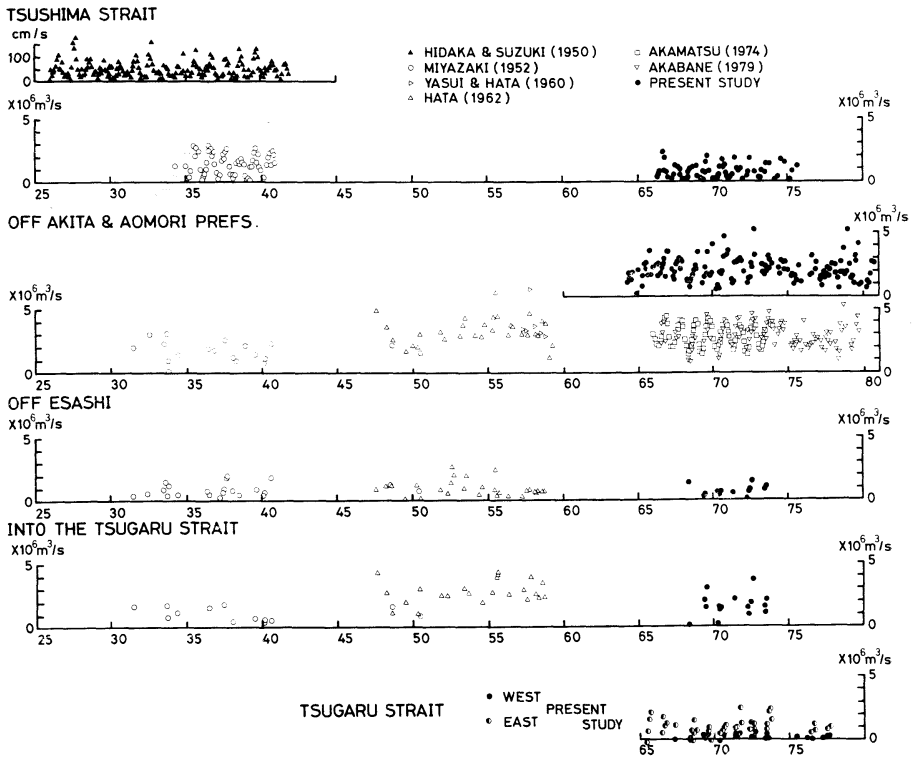

Fig. 2. Synthetic time series from Table 1.

reference level of 300 db, together with an assumption that the waters warmer than 7°C constitute the transport of the warm current following the proposal by MIYAZAKI (1952). The transport estimated by use of Q-value defined by

$$Q=\int_0^R (\Delta D_R-\Delta D_Z)dz$$

is also entered by closed triangles, where ΔD_R and ΔD_Z are the dynamic depth anomaly from the surface to the depth of R and Z, respectively, and R is the assumed layer of no motion. The

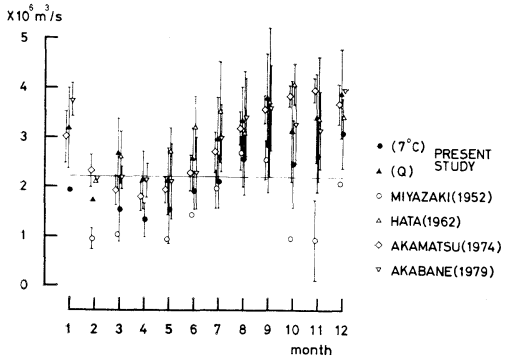

Fig. 3. Seasonal variability of the warm current system estimated off Akita and Aomori Prefectures.

Q-values for two stations A and B are correlated with the volume transport V through a section between A and B by

$$V=f^{-1}(Q_A-Q_B)$$

where f is the Coriolis parameter. It is naturally larger than the transport above 7°C.

In the present study the current transport has been calculated by use of available data from 1965 to 1977, obtained by Fisheries Experiment Stations of Aomori and Akita Prefectures. The overall feature is characterized by the minimum in February through May, and the maximum in August through September. The annual average is estimated as $2.2\times10^6 m^3 s^{-1}$ with a range of variation of $1.6\times10^6 m^3 s^{-1}$, from the present data. The value for December is rather large, but the reason is yet to be elucidated.

The reason for choosing 7°C as the criterion of warm water is qualitatively substantiated by the temperature sections shown in Fig. 4, of which the location of stations indicated at the top is shown in Fig. 5. The second thermocline is seen around 7°C in (a) for the section off Aomori, and it approximately corresponds to the sill depth of the west entrance of the Tsugaru Strait, as seen in (b). The sectional area above 7°C at the section off Esashi shown in (c) is much smaller than that shown in (a),

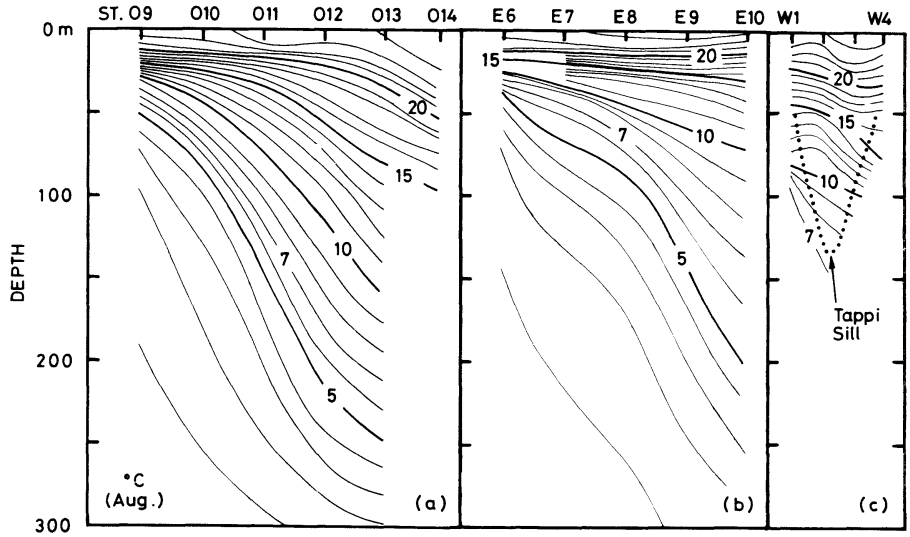

Fig. 4. Temperature section to the south (a), to the north (b), and at the entrance (c) of Tsugaru Strait. For location of stations, see Fig. 5.

indicating that most of the water above 7°C flows out through the Tsugaru Strait. The T-S diagrams shown in Fig. 6 also support the above criterion. Namely, the water entering the Tsugaru Strait (b) has a temperature warmer than 7°C, and the water just to the north of the Strait (c) has almost the same characteristics as the water proper to the Japan Sea (d).

Fig. 7 shows the baroclinic geostrophic transport estimated at Tsushima Strait at its mouth of the Japan Sea side. The present estimate, obtained by use of data from Yamaguchi Prefecture Open-Sea Fish. Exp. Station, is indicated by solid circles with error limits. Since the observation line did not reach the Korean coast, the values are about 70% of the estimates by MIYAZAKI (1952) and by YI (1966) who used sections covering the entire Strait. The pattern of the seasonal variation is characterized by minimum in February through April and maximum in July through November, and using values by MIYAZAKI (1952) and YI (1966) the average transport is estimated as 1.3×10^6 m^3s^{-1} with the annual range of $2.0\times10^6 m^3s^{-1}$. Since the value is much smaller than the above estimated transport off Akita-Aomori, it is inferred that the barotropic geostrophic or ageostrophic components do exist at the Strait, especially in winter through spring. This inference agrees with MIIDA's (1976) observation from direct current measurements in the Strait in summer.

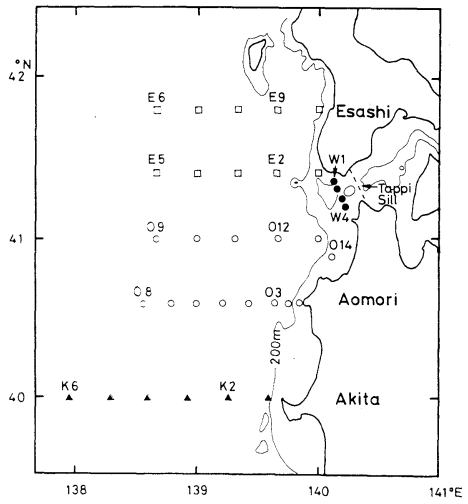

Fig. 5. Location of stations for Figs. 4 and 6.

It should be noted here that, according to MIYAZAKI (1952), the ratio of the transports between the west part (Korea Strait) and the east part of the Strait is 3:1.

Fig. 8 shows the baroclinic geostrophic transport at the west and the east mouths of Tsugaru

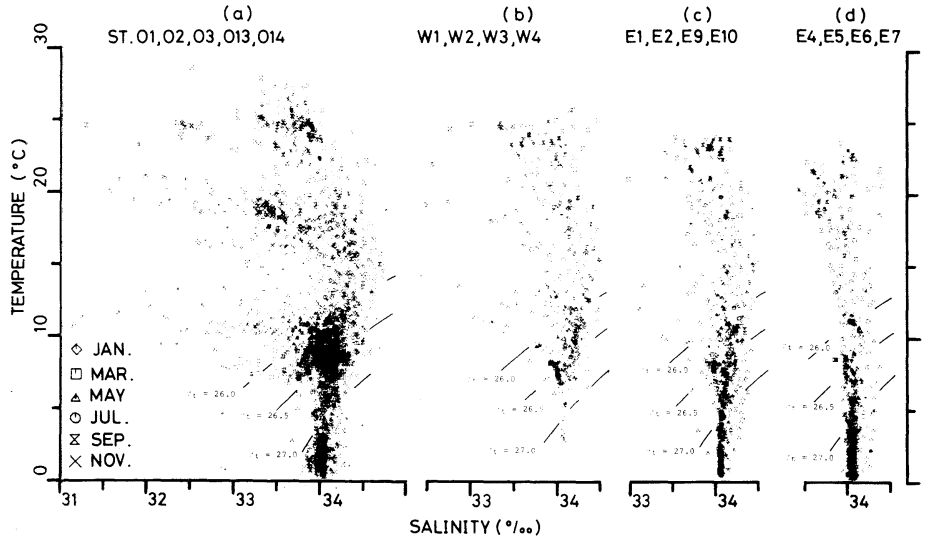

Fig. 6. T-S diagram for waters to the south (a), at the entrance (b), to the north (c) of Tsugaru Strait, and for the water proper to the Japan Sea (d). For location of stations, see Fig. 5.

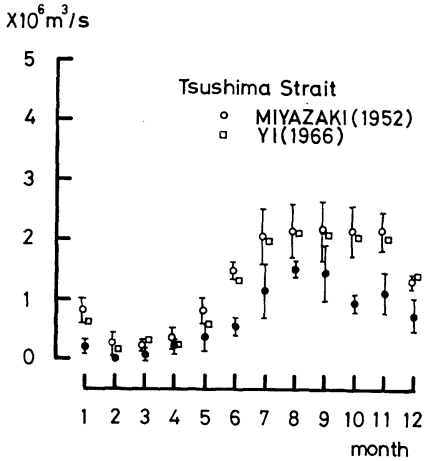

Fig. 7. Baroclinic geostrophic transport at Tsushima Strait, at the mouth of the Japan Sea side (see the text).

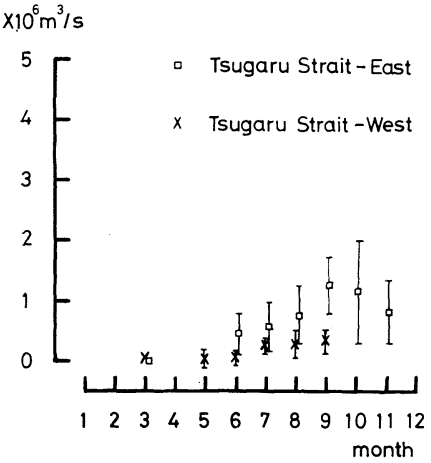

Fig. 8. Baroclinic geostrophic transport at west and east mouths of Tsugaru Strait.

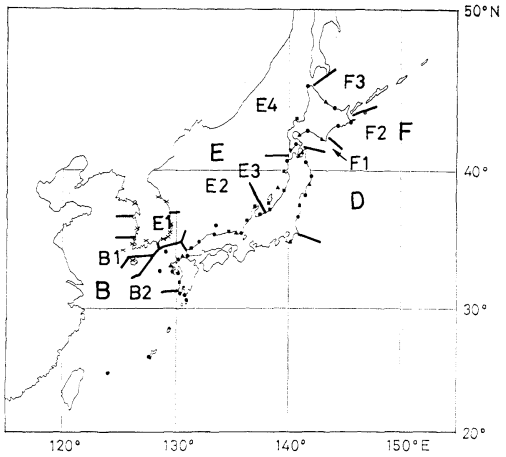

Fig. 9. Tidal stations, and sub-regions of the sea defined from the characteristics of tidal records (see the text).

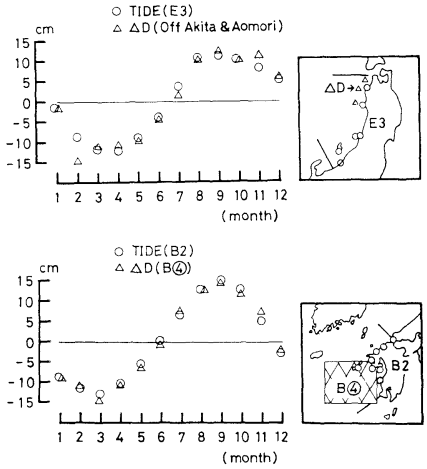

Fig. 10. Examples of comparison between tidal variation and ΔD variation.

Strait, obtained by use of data provided by Fish. Exp. Stations of Hakodate and Aomori Pref. It is inferred that the component other than baroclinic geostrophic transport is much larger here, especially at the west part of the Strait. The pattern of seasonal variation seems similar to that of the Tsushima Strait.

The year-to-year variability will be discussed in section 4.

3. Comparison with sea level variability—the origin of the current variability

Monthly mean tidal records, at stations shown in Fig. 9 along the coasts of Japan and Korea, have been treated. Corrections for atmospheric pressure, and for the crustal deformation assumed by a linear trend, have been applied. Patterns of variability of the sea level thus obtained for these stations have made it possible for us to define several sub-regions of the sea, where the pattern of variation of the sea level may be regarded as similar within the respective sub-regions, as shown also in Fig. 9. The detailed description of this part of treatment will be published elsewhere by TOMIZAWA *et al.*

The variation of the sea level averaged over

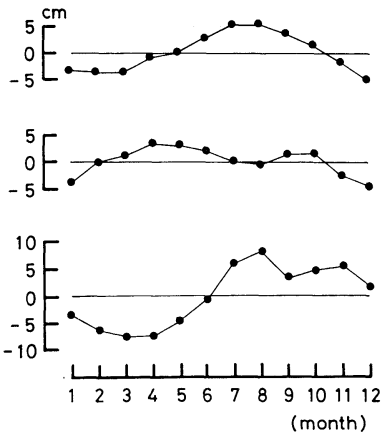

Fig. 11. Seasonal variation of sea level differences at Tsushima Strait. Top: in current direction along Korean coast; middle: same except along Japanese coast; bottom: across the Strait.

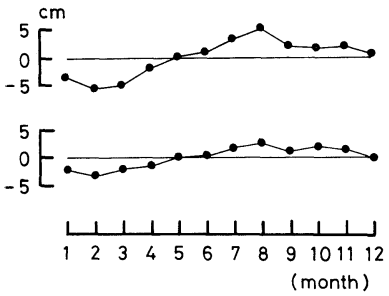

Fig. 12. Seasonal variation of sea level differences at Tsugaru Strait. Upper: in the current direction; lower: across the Strait.

the sub-regions may be closely correlated with the dynamic depth anomaly ΔD near the coast, which can be obtained from hydrographic data. Some examples of the comparison between tidal variation and ΔD variation are shown in Fig. 10. It should be noted that, if a comparison is made between ΔD far off the coast and tidal value, the correspondence is not necessarily close.

Fig. 11 shows types of seasonal variation of three kinds of sea level differences at the Tsushima Strait in relative values. The sea level difference in current direction may be regarded as representing the cause of the flow through the strait, whereas the difference across the strait is related to the degree of attainment of geostrophic balance. The top figure is the sea

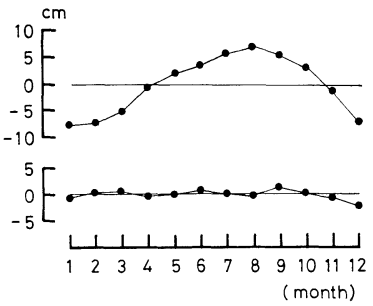

Fig. 13. Seasonal variation of sea level differences. Upper: between East China Sea and sea area east of Tsugaru; lower: between entrance and exit of the Japan Sea.

level difference in the current direction along the Korean coast, i.e., between B1 and E1 in Fig. 9, the middle figure that along the Japanese coast, between B2 and E2, and the bottom figure is the difference across the Strait, between E2 and E1. Since the majority of the transport of the Tsushima Current flows through the Korea Strait as mentioned previously, we regard the top figure rather than the middle one as the sea level difference in current direction. The annual range is 10 cm. The bottom figure shows a similar trend.

Fig. 12 concerns the sea level differences at the Tsugaru Strait. The upper figure is the difference in the current direction, i.e., between the mean value of E3 and E4 and that of D, F1 and F2, and the lower is the difference across the Strait (between the mean level of Asamushi-Ominato and Hakodate). The shapes of the curves are similar to the top figure of Fig. 11. The annual range of difference in current direction is here also 10 cm.

The upper part of Fig. 13 shows the variation of sea level difference between the East China Sea and the sea areae ast of Tsugaru, i.e., between the average value of B1 and B2 and that of D, F1 and F2, while the lower part shows the difference between the entrance and the exit of the Japan Sea, i.e., between the average level of E1 and E2 and that of E3 and E4, in relative values.

The upper part of Fig. 13 has a similar shape to Figs. 11 and 12, but the lower part shows no definite trend of seasonal variation; consequently the upper represents approximately

the sum of the top figures of Figs. 11 and 12. The upper part of Fig. 13 is also quite similar to the seasonal variation of ΔD-difference between the East China Sea and the sea area east of Tsugaru as shown in Fig. 14. The range of annual variation is about 15 cm for both.

From Figs. 11, 12 and 13, it can be seen that the sea level inside the Japan Sea is in an equilibrium state in a time scale of seasonal variability, though it does not mean that the Japan Sea is always in stationary level because we have treated only relative values of variation at each sub-region.

The pattern of seasonal variation of sea level difference outside the Japan Sea, represented by the upper part of Fig. 13, is quite similar to that of the volume transport of the Warm Current System shown in Fig. 3, except that the latter has a delay of phase of one to two months. One of the causes of the phase lag may be attributed to the process of taking the monthly mean, especially taking discrete hydrographic observations, but other causes will be more complicated, probably including relaxation of the system, or inertia of the circulating part of the current within the Japan Sea.

The range of variation of sea level difference of 10 cm in current direction at the Tsushima and the Tsugaru Straits should correspond to the annual range of the warm current transport of about $2\times10^6 m^3 s^{-1}$. Since the mean absolute value of the transport is also $2\times10^6 m^3 s^{-1}$, the mean absolute sea level differences will also be 10 cm for both the straits, if a linear relation is assumed. It is easy to verify that the transport of $2\times10^6 m^3 s^{-1}$ corresponds reasonably in order of magnitude to the sea level difference of 10 cm at these straits, if we assume a balance between the pressure gradient in the current direction and bottom friction, with a value of friction factor, proportional to the mean current velocity as used by KNAUSS (1978), of 1×10^{-5} s^{-1} for 1×10^2m of the mean depth.

Thus it is concluded that the seasonal variability of the Tsushima-Tsugaru Warm Current System is primarily controlled by the variability of sea level difference between the East China Sea and the sea area east of Tsugaru. In the former sea the variation of sea level is large owing to the seasonally varying effective air-sea heat exchange, since the sea is shallow and is located at the margin of the continent where the monsoon prevails over the sea in winter season, and in the latter sea area the air-sea heat exchange is rather small, and the sea level is much controlled by conditions of the cold subarctic gyre.

4. Year-to-year variability

The conclusion derived for the seasonal vari-

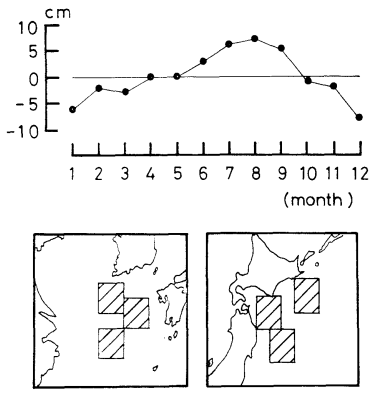

Fig. 14. Seasonal variation of ΔD-difference between East China Sea and the sea area east of Tsugaru, in relative values. Sea areas for the estimation of ΔD's are shown by shaded areas. From data by KURASAWA (1980).

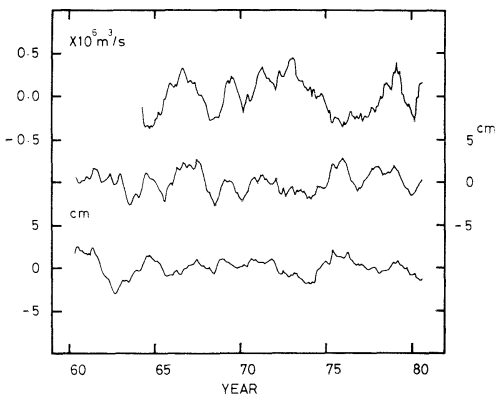

Fig. 15. Year-to-year variability of the transport of the Warm Current System (top), sea level difference between the East China Sea and the sea area east of Tsugaru (middle), and sea level difference between entrance and exit of the Japan Sea.

ability is checked further for year-to-year variability. The top graph of Fig. 15 represents the time series of transport of the Warm Current System evaluated off Akita and Aomori Prefectures, corresponding to Fig. 3. The graph has been plotted by taking a thirteen-month moving average after the mean annual variation was subtracted from the original monthly values. There are two to five months in a year when data are not available. For these particular months, values for mean seasonal variation have been inserted. Values for 1974 to 1976 are especially unreliable for this reason. The middle graph is a time series of the sea level differences between the East China Sea and the sea area east of Tsugaru, corresponding to Fig. 13. The bottom graph is the variation of sea level difference between the entrance and the exit of the Japan Sea, corresponding also to Fig. 13. Here also, thirteen-month average values are plotted, after the crustal deformation assumed by a linear trend for the whole period of the analysis is subtracted.

It is seen that the correlation between the top and the middle figures is good for a variability of two or three years, and it is especially close for the period 1964 to 1971, supporting the same conclusion with the case of seasonal variation. On the other hand, disagreement in variability with longer periods of about several years is seen. It is especially conspicuous from 1972 to 1978. However, in the analysis of year-to-year variability, the effect of crustal deformation is crucial, and cannot reasonably be eliminated from the tidal records. So the reason of the above disagreement might be attributed to the assumption of the linear trend crustal deformation applied for each tide station.

The sea level difference within the Japan Sea shown in the bottom figure seems comparable in order of magnitude to that outside the Japan Sea shown in the middle figure, in contrast to Fig. 13. However, it is understandable since the range of variability of the middle figure is originally small compared to the seasonal one by a factor of 3, and the effect of crustal deformation must be included here also.

5. Formula for volume transport

In the preceding sections, it has been concluded that the variability of the Warm Current System in the Japan Sea is controlled by the difference of sea level or ΔD between the East China Sea and the sea area east of Tsugaru.

Several numerical values obtained in Section 3 may be synthesized to get a self-consistent picture as shown in Fig. 16, if a linear relation is assumed. The figure is drawn in reference to the sea level of the sea area east of Tsugaru. The slope within the Japan Sea is unvaried, but the absolute value is unknown, and it is drawn here with an arbitrary slope.

The plausible values are: the average sea level difference along both the Tsushima and Tsugaru Straits is 10 cm with an annual range of 8 cm; the annual range of the sea level (or ΔD) difference between the East China Sea and the sea area east of Tsugaru is 16 cm; and the average volume transport of the Warm Current System is $2.0\times10^6 m^3 s^{-1}$ with an annual range of $1.6\times10^6 m^3 s^{-1}$. Thus we propose a formula between the volume transport V and the deviation from the average of the sea level difference between the East China Sea and the area east of Tsugaru ΔH:

$$V(10^6 m^3 s^{-1}) = 2.0 + 0.1\,\Delta H\,(\mathrm{cm}).$$

Though this has been derived from the analysis of seasonal variation, it may also be applicable to year-to-year variability, as is checked by Fig.

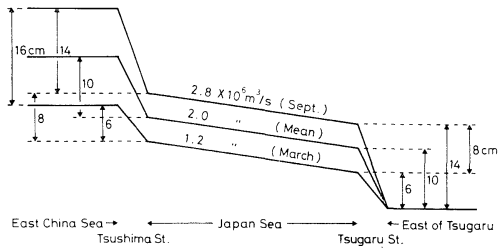

Fig. 16. A synthesized picture of the relationship among sea levels and volume transport of the Warm Current System. The sea level is drawn in reference to sea area east of Tsugaru. The slope within the Japan Sea is drawn with an arbitrary slope, since the slope is unvaried, though the absolute value is unknown.

15 for the period of 1964 to 1971. For seasonal variability, there is a delay of phase of one to two months in the volume transport.

Acknowledgments

The authors wish to express their thanks to various organizations which kindly provided observational data, especially to the Japan Oceanographic Data Center; Fisheries Experiment Stations of Akita, Aomori, and Yamaguchi Prefectures and of Hakodate; Geophysical Survey Institute of Japan, and the Hydrographic Office of Korea. They also thank Prof. Y. HSUEH of Florida State University for his comments to the first manuscript, and Mrs. M. Heather KOTAKE for her correction of the sentences. The study was partially supported by the Grant-in-Aid for Scientific Research from the Ministry of Education, Science and Culture, (Special Project Research, The Ocean Characteristics and their Changes, Project No. 56217004). The numerical calculations were carried out on an ACOS-900 of the Computer Center of Tohoku University.

References

AKABANE, M. (1979): The variabilities of hydrographic conditions of the Tsugaru Warm Current from the viewpoint of volume transport. Abstract of paper presented at 29th Tohoku Area Oceanic Survey Technical Conference, 12 pp. (in Japanese).

AKABANE, M., M. TAMURA and K. TAKANASHI (1979): Water-mass distribution and flows in the Tsushima Warm Current region. *In* Report of Synthetic Studies on the Tsugaru Warm Current Region. The Science and Technology Agency, 228-236 (in Japanese).

AKAMATSU, H. (1974): On the variability of hydrographic conditions in the Japan Sea from the viewpoint of heat consumption. Abstracts of papers, Symposium on Long-term Variabilities of Hydrographic Conditions, JMA, 18-24 (in Japanese).

AKAMATSU, H. (1977): On the origin of the Tsushima Warm Current. Abstracts of papers, Autumn Meeting of Oceanogr. Soc. Japan, 1977, 233-234 (in Japanese).

AOTA, M. (1975): Studies on the Soya Warm Current. Low Temperature Science, Ser. A, **33**, 151-172 (in Japanese).

CONLON, D. M. (1981): Dynamics of flow in the region of the Tsushima Strait. Coastal Studies Institute, Louisiana State Univ., Technical Report No. 312, 62 pp.

HATA, K. (1962): Seasonal variation of the volume transport in the northern part of the Japan Sea. J. Oceanogr. Soc. Japan, 20th Anniv. Vol., 168-179 (in Japanese).

HATA, K. (1973): Variations in hydrographic conditions in the seas adjacent to the Tsugaru Straits. J. Meteor. Res., **25**, 467-479 (in Japanese).

HIDAKA, K. and T. SUZUKI (1950): Secular variation of the Tsushima Current. J. Oceanogr. Soc. Japan, **6**, 28-31 (in Japanese).

JAPAN METEOROLOGICAL AGENCY (1979): The characteristics of oceanic structures in the Tsugaru Warm Current region and explanation of relations between hydrographic and meteorological variabilities. Report of Synthetic Studies on the Tsugaru Warm Current Region. The Science and Technology Agency, 99-222 (in Japanese).

KIMURA, Y. (1978): The current transport and its variations in the Japan Sea. Abstracts of papers, Autumn Meeting of Oceanogr. Soc. Japan, 1978, 44-45 (in Japanese).

KNAUSS, J. A. (1978): Introduction to Physical Oceanography. Prentice Hall, 338 pp.

KURASAWA, Y. (1980): Oceanic variation of regional seas in tne northwestern Pacific Ocean and its relation to current variability around Japan. M. Sc. Thesis of Tohoku University (in Japanese).

KUSUNOKI, H. and T. KASHIMA (1951): Ocean current variation off the western coast of Hokkaido in the Japan Sea. J. Oceanogr. Soc. Japan, **6**, 133-142 (in Japanese).

MIIDA, T. (1976): Flows from anchored current measurements. Bull. Japan. Soc. Fish. Oceanogr., **28**, 33-58 (in Japanese).

MINATO, S. and R. KIMURA (1980): Volume transport of the western boundary current penetrating into a marginal sea. J. Oceanogr. Soc. Japan, **36**, 185-195.

MIYAZAKI, M. (1952): The heat budget in the Japan Sea. Bull. Hokkaido Reg. Fish. Res. Lab., **4**, 1-45 (in Japanese).

MORIYASU, S. (1972): The Tsushima Current. *In* Kuroshio, its Physical Aspects (H. STOMMEL and K. YOSHIDA, ed.) Univ. of Tokyo Press, p. 353-369.

SUDA, K. (1938): Annual variation of the Tsushima Current. Japan. J. Limnol., **8** (Dr. Tanaka's Seventieth Anniversary Vol.), 205-216.

SUGIURA, J. (1958): On the Tsugaru Warm Current. Geophys. Mag., **28**, 400-409.

YASUI, Z. and K. HATA (1960): On the seasonal

variations of the sea conditions in the Tsugaru Warm Current region. Mem. Kobe Mar. Obs., **14**, 3-12.

YI. S. U. (1966): Seasonal and secular variations of the water volume transport across the Korea Strait. J. Oceanogr. Soc. Korea, **1**, 7-13.

対馬・津軽暖流系の季節変化・経年変動とその可能な原因

鳥羽良明，富沢和身，倉沢由和，花輪公雄

要旨：日本海に出入りする海流は，1カ月以上の時間スケールでは流出入量がバランスしているとみなせる。対馬暖流と津軽暖流とを日本海を通過する主な暖流系とみなし，過去に蓄積された資料を総合して，その季節変化・経年変動の最も確からしいイメージを求め，その変動の起源を追求した。体積輸送の平均的季節変化の特徴は，2月から5月に最小，8月，9月に最大で，年平均は $2.0\times10^6 m^3 s^{-1}$，変動幅は $1.6\times10^6 m^3 s^{-1}$ である。この暖流系は，大気海洋相互作用によって水温変動の大きい東シナ海と，冷たい亜寒帯環流の西端である津軽東方海域との間の水位差すなわち ΔD の差によって駆動され，制御されていることが推論された。定量的には次の公式を提出する。すなわち，$V(10^6 m^3 s^{-1})=2.0+0.1\Delta H$(cm)。ここに V は暖流系の体積輸送，ΔH は東シナ海と津軽東方海域との水位差の平均値からの偏差であり，季節変化については，体積輸送に1，2カ月の位相の遅れがある。

お　知　ら　せ

2nd JECSS Workshop について

JECSS は "Japan and East China Seas Study" の略である。1981 年 6 月 1 日から 4 日まで筑波大学で開かれた 1st JECSS Workshop でのとりきめにしたがい，2nd JECSS Workshop が来年 1983 年（おそらく 4 月）に開かれる。場所は東京近辺となろうが今のところ未定である。前回とほぼ同じく，Workshop のおもな目的は，(1) 日本海・東シナ海の海況の研究状況を見わたすこと，(2) これらの海をとりまく国々およびアメリカの研究者の間の研究協力を推進すること，である。物理に重点がおかれているとはいえ，化学や地質なども含まれることも前回と同じである。

今回は，アメリカ・中国の黄海協同研究や韓国・アメリカの朝鮮海峡協同研究も話題になりそうであり，また，対象を南シナ海にまでひろげた MIDAS/JEASUS (Multinational Investigation of Development of Adjacent Seas/Japan and East Asian Seas Unified Study) も検討されるかも知れない。

昨年の Workshop は，会場や宿舎などの準備に日がなくて，不手ぎわがすくなくなかったが，それでも参加者の多くによれば成功だった。来年のはさらによく運営されるだろう。

この会についての照会先は，〒305 茨城県新治郡桜村 筑波大学生物科学系 高野健三（電話は 0298-53-6682, 4651）である。　（高 野 健 三）

お　詫　び

昭和 56 年 11 月 30 日付で本学会創立 20 周年記念事業決算報告を醵金者の方がたに送付いたしましたが，同報告の醵金者御芳名中に

三 井 海 洋 開 発 ㈱

が脱落しておりました。ここに不手際を衷心からお詫びいたします。

日 仏 海 洋 学 会

学 会 記 事

1. 昭和56年12月２日　東京水産大学において昭和57年度学会賞受賞候補者推薦委員会(第１回)が開かれた。

2. 昭和56年12月19日　東京水産大学において編集委員会が開かれ，La mer 第20巻第１号の編集を行った。

3. 昭和56年12月23日　東京水産大学において昭和57年度学会賞受賞候補者推薦委員会(第２回)が開かれ，審議の結果，候補者として鎌谷明善氏を推薦することとし，この旨井上実委員長から会長に報告された。

4. 昭和57年１月29日　日仏会館会議室において日仏会館と日仏関連諸学会との懇談会が開かれ，本学会からは佐々木忠義会長，有賀祐勝常任幹事，佐伯和昭庶務幹事，高野健三幹事が出席した。

5. 新入会員

氏　名	所　属	紹介者
(正会員)		
三村　徹	Université d'AIX-Marseille II	八木　宏樹
松本宗治	〒666 川西市美園町3-11	佐々木忠義
今関昭博	東京水産大学	松生　洽
櫻本和美	東京水産大学	松生　洽
姜　憲	筑波大学　生物研究科	関　文威
杉田治男	日本大学農獣医学部 水産学科	吉田　陽一
原田邦二	University of Sydney	有賀　祐勝
CARLES, Didier	Université d'AIX-Marseille II	三村　徹
(賛助会員)		
㈱読売広告社	〒104 中央区銀座1-8-14	

6. 退会者

関川　正，杉浦吉雄，早川康信，橘高重義，関　晋

8. 会員の住所・所属の変更

氏　名	新住所または新所属
菅野　尚	〒104 中央区勝どき5-5-1 東海区水産研究所企画連絡室

7. 交換および寄贈図書

1) 農業土木試験場　場報　Nos. 31, 32
2) 農業土木試験場報告，技報論文要約集　第８号
3) 海洋産業研究資料　Vol. 12 No. 9
4) 養殖研ニュース　No. 2
5) 高知大学　海洋生物教育研究センター 研究報告　No. 3
6) 研究実用化報告　Vol. 30 Nos. 10, 11, 12, Vol. 31 Nos. 1, 2
7) 広島県水産試験場研究報告　第11号
8) 海洋時報　第23号
9) 国立科学博物館研究報告　Vol. 7 No. 3
10) 鯨研通信　341, 342, 343号
11) 広島日仏協会報　No. 81
12) 日本航海学会論文集　第65号
13) 日本海区水産研究所報告　第32号
14) なつしま　Nos. 55, 56
15) 海上気象報告　37号
16) 航　海　第70号
17) 函館海洋気象台要報　第20号
18) 海洋科学技術センター　十年史
19) 出版物目録（農業土木試験場）
20) 広島大学生物生産学部紀要　第20巻第２号
21) 横須賀市立博物館研究報告　第28号
22) 海洋資料センター要覧
23) 東北区水産研究所研究報告　43号
24) 釜山水産大学研究報告　第13巻
25) Recueil des Travaux　Vol. XVII 1980
26) 科学通報　Vol. 26 No. 12, Vol. 27 No. 1

評議員　青山恒雄，赤松秀雄，秋山　勉，阿部宗明，
阿部友三郎，新崎盛敏，有賀祐勝，石野　誠，
石渡直典，市村俊英，井上　実，今村　豊，
入江春彦，岩崎秀人，岩下光男，岩田憲幸，
宇田道隆，宇野　寛，大内正夫，小倉通男，
大村秀雄，岡部史郎，岡見　登，梶浦欣二郎，
加藤重一，加納　敬，川合英夫，川上太左英，
川村輝良，川原田　裕，神田献二，菊地真一，
草下孝也，楠　　宏，国司秀明，久保田　穣，
黒木敏郎，小泉政美，小林　博，小牧勇蔵，
西条八束，斎藤泰一，斎藤行正，佐伯和昭，
坂本市太郎，　佐々木忠義，　佐々木幸康，
猿橋勝子，柴田恵司，下村敏正，庄司大太郎，
関　文威，多賀信夫，高木和徳，高野健三，
高橋淳雄，高橋　正，谷口　旭，田村　保，
千葉卓夫，辻田時美，寺本俊彦，鳥羽良明，
冨永政英，鳥居鉄也，中井甚二郎，中野猿人，
永田　正，永田　豊，奈須敬二，奈須紀幸，
西沢　敏，根本敬久，野村　正，半沢正男，
半谷高久，樋口明生，菱田耕造，日比谷　京，
平野敏行，深沢文雄，深瀬　茂，福島久雄，
淵　秀隆，増沢譲太郎，増田辰良，松生　洽，
丸茂隆三，三浦昭雄，三宅泰雄，村野正昭，
元田　茂，森川吉郎，森田良美，森安茂雄，
安井　正，柳川三郎，山路　勇，山中鷹之助，
山中一郎，山中　一，吉田多摩夫，渡辺精一
（五十音順）
マルセル・ジュグラリス，ジャン・アンクティル，ロジェ・ペリカ

賛　助　会　員

旭化成工業株式会社	東京都千代田区有楽町 1-1-2　三井ビル
株式会社内田老鶴圃新社　内田悟	東京都千代田区九段北 1-2-1　蜂谷ビル
株式会社　オーシャン・エージ社	東京都千代田区神田美土代町 11-2　第1東英ビル
株式会社　大　林　組	東京都千代田区神田司町 2-3
株式会社　オセアノート	東京都世田谷区北沢 1-19-4-202
小樽舶用電機株式会社	小樽市色内町 3-4-3
株式会社　オルガノ	東京都文京区本郷 5-5-16
社団法人　海洋産業研究会	東京都港区新橋 3-1-10　丸藤ビル
協同低温工業株式会社	東京都千代田区神田佐久間町 1-21　山伝ビル
小松川化工機株式会社	東京都千代田区岩本町1-10-5　TMMビル5F
小　山　康　三	東京都文京区本駒込 6-15-10　英和印刷社
三信船舶電具株式会社	東京都千代田区神田 1-16-8
三洋水路測量株式会社	東京都港区新橋 5-23-7　三栄ビル
シュナイダー財団極東駐在事務所	東京都港区南青山 2-2-8　DFビル
昭和電装株式会社	高松市寺井町 1079
新日本気象海洋株式会社	東京都世田谷区玉川 3-14-5
株式会社　鶴見精機	横浜市鶴見区鶴見中央 2-2-20
株式会社　東京久栄	東京都中央区日本橋 3-1-15　久栄ビル
東京製綱繊維ロープ株式会社	東京都中央区日本橋室町 2-6　江戸ビル
株式会社　東邦電探	東京都杉並区宮前 1-8-9
中川防蝕工業株式会社	東京都千代田区神田鍛冶町 2-2-2　東京建物ビル
日本アクアラング株式会社	神奈川県厚木市温水 2229-4
日本テトラポッド株式会社	東京都港区新橋 2-1-13　新橋富士ビル9階
社団法人　日本能率協会	東京都港区芝公園 3-1-22　協立ビル
日本プレスコンクリート株式会社	東京都中央区日本橋本石町 1-4
深田サルベージ株式会社	東京都千代田区神田錦町 1-9-1　天理教ビル8階
藤　田　　潔	東京都新宿区四谷 3-9　光明堂ビル　株式会社ビデオプロモーション
藤　田　峯　雄	茨城県北相馬郡藤代町大字毛有 850　株式会社 中村鉄工所
古野電気株式会社	東京都中央区八重洲 4-5　藤和ビル
丸文株式会社	東京都中央区日本橋大伝馬町 2-1-1
三井海洋開発株式会社	東京都千代田区一ツ橋 2-3-1　小学館ビル
宮　本　　悟	東京都中央区かちどき 3-3-5　かちどきビル　㈱ 本地郷
株式会社ユニオン・エンジニアリング　佐野博持	神戸市中央区海岸通 3-1-1 KCCビル4F
吉野計器製作所	東京都北区西ケ原 1-14
株式会社読売広告社	東京都中央区銀座 1-8-14
株式会社　離合社	東京都千代田区神田鍛冶町 1-10-4
株式会社　渡部計器製作所	東京都文京区向丘 1-7-17

Exploiting the Ocean by...

T.S.K.
OCEANOGRAPHIC INSTRUMENTS

REPRESENTATIVE GROUPS OF INSTRUMENTS AND SYSTEMS

T.S- 塩分計 DIGI-AUTO 《新製品》

本器は電磁誘導方式による卓上塩分計として画期的な T.S-E シリーズを全自動化した新製品です。その取扱いには熟練を必要とせず，誰にでも迅速・容易・正確に塩分値を計測する事が出来ます。

◎ 資料の海水ビンにチューブを入れてスタートボタンを押すだけで自動的に作動し塩分値を表示し又速かに試水は元にもどります。
◎ 大型 LED デジタル表示
◎ 高精度・高安定度
◎ 検出部にサンプルの吸入速度を自動的にコントロールしているのでセル部への気泡付着に気を使う必要はありません。
◎ 電極式ではないため洗浄等のメンテナンスも容易です。
◎ 二重の安定装置によりポンプの寿命がのびました。

測定範囲	0～36 ‰ S
精度	±0.01 ‰ S
分解能	0.001 ‰ S
自動温度補償範囲	5～30° C
所要試水量	約 60 cc
電源	AC 100V 50/60Hz
重量	約 15 kg
寸法	450×250×400m/m

株式会社 **鶴見精機**

横浜市鶴見区鶴見中央2丁目2番20号 〒230 TEL; 045-521-5252

CABLE ADDRESS; TSURUMISEIKI Yokohama, TELEX; 3823750 TSKJPN J

OVERSEAS OFFICE; TSK-AMERICA INC. Seattle WASHINGTON

IWAMIYA INSTRUMENTATION LABORATORY

昭和 57 年 2 月 25 日 印刷
昭和 57 年 2 月 28 日 発行

う み

第 20 巻
第 1 号

定価 ¥ 1,200

編集者 冨永政英
発行者 佐々木忠義
発行所 日仏海洋学会
財団法人 日仏会館内
東京都千代田区神田駿河台2-3
郵便番号：1 0 1
電話：03(291) 1 1 4 1
振替番号：東京 5-96503

印刷者 小山康三
印刷所 英和印刷社
東京都文京区本駒込 6-15-10
郵便番号：1 1 3
電話：03(941) 6 5 0 0

Tome 20　　N° 1

SOMMAIRE

第 20 巻　　第 1 号

目　　次